

https://dspace.org/

Investigating hypoxia inducible factor-1 alpha as a putative regulator of peroxidasin

Niyobuntu, Eunice

2021

https://hdl.handle.net/10539/32477

Downloaded from a DSpace repository. https://dspace.org/

INVESTIGATING HYPOXIA INDUCIBLE FACTOR-1 ALPHA AS A PUTATIVE REGULATOR OF *PEROXIDASIN*

Eunice Niyobuntu (903879)

Supervisor: Prof Demetra Mavri-Damelin

A dissertation submitted to the Faculty of Science, University of the Witwatersrand, in fulfilment of the requirements for the degree of Master of Science.

Johannesburg, 2020

I, **Eunice Niyobuntu (903879)**, am a student registered for the degree of **MSc (dissertation) in Biological Science** in the academic year **2020.**

I hereby declare the following:

- I am aware that plagiarism (the use of someone else's work without their permission and/or without acknowledging the original source) is wrong.
- I confirm that the research proposal submitted for assessment for the above degree is my own unaided work except where explicitly indicated otherwise and acknowledged.
- I have followed the required conventions in referencing the thoughts and ideas of others.
- I understand that the University of the Witwatersrand may take disciplinary action against me if there is a belief that this is not my own unaided work or that I have failed to acknowledge the source of the ideas or words in my writing.

Signature: 

ABSTRACT

Peroxidasin is a mammalian haem-peroxidase that, unlike other mammalian haem peroxidases, contains additional motifs characteristic of extra-cellular matrix (ECM) proteins. This feature allows for the speculation that PXDN may have other functions within the ECM in addition to its catalytic activity. One such function is the crosslinking of collagen IV in the ECM – a crucial process for basement membrane integrity. Whilst normally expressed in the cardiovascular system and eye, dysregulated PXDN expression is observed in multiple human diseases including fibrosis and cancer. The role of hypoxia in the development and progression of such disease phenotypes has already been elucidated, therefore we hypothesised that *pxdn* may be regulated by HIF-1α is the master regulator of the cellular response to hypoxia, controlling the expression of approximately 200 genes once active. To accomplish this, localisation and protein quantification of PXDN and HIF-1α were observed in HeLa cells treated with cobalt chloride ($CoCl_2$) using immunofluorescence confocal microscopy and Western blot, respectively. Both HIF-1α and PXDN show increased protein expression in response to treatment with 100μM $CoCl_2$, a hypoxia mimetic, over a 24-hour period. PXDN expression was observed in the ECM and HIF-1α in the nucleus, as expected. The interactions between HIF-1α and the *pxdn* promoter region were then observed using chromatin immunoprecipitation and PCR. HIF-1 binds the *pxdn* promoter at a region 741bp and 801bp upstream of the transcription start site. This data shows that, in the presence of $CoCl_2$, HIF-1α and PXDN expression is increased in cervical cancer cells and we also show that HIF-1α interacts with the *pxdn* promoter. However further work should be carried out to determine whether this interaction between HIF-1α and *pxdn* drives transcription. Understanding the interactions between HIF-1α and PXDN may lead to the development of novel therapeutic targets for cancer and other diseases where PXDN and HIF-1α are implicated.

For God and for my family.

ACKNOWLEDGEMENTS

First, my deep gratitude goes to my supervisor Prof Demetra Mavri-Damelin. The research done in this dissertation is her very own design and I have enjoyed how being a part of this work has developed in me the foundation for critical thinking, writing and research. Moreover, I would like to thank the Functional Genetics Research Group. Over the past 3 years, I have been blessed to meet other budding scientists that have been an integral part of my understanding and progress. Dr Rupal Jivan, Dr Kerry Hanmer, Dr Boitumelo Sitole, Mr Tebogo Marutha and Mr Ntakadzeni Nemuvumoni; thank you for the knowledge and assistance you afforded me during my time at Gate House.

I must thank the National Research Foundation (NRF) for funding me throughout my MSc years. I acknowledge the School of Molecular and Cell Biology which has been my learning grounds for the past 6 years. I have grown with MCB and I am grateful that I was taught under such brilliant lecturers and that I have met a number of inspiring individuals, some who have become friends now. I am grateful for the teaching opportunities and the many students I have encountered by being a TA and for the always kind and helpful staff.

My family has always been a wellspring of support for me, but I have come to understand this all the more during my postgraduate years. I thank my mother always; it would not be a lie to say that I have written this because of her grace and wisdom poured over me throughout my lifetime. My siblings who have continued to protect and support me did no less in this time. I would like to especially thank my brother Eliezer for his constant encouragement, not just in words but in action, I believe he understands what this means. I cannot forget my extended family and friends for all the calls and words of encouragement, these meant more than I ever expressed.

Finally, I must thank God who has been the source and inner strength for me in my day to day during these past 2 years. Without this faith and hope, I would not have been able to withstand and overcome the failures and growth that come with being a researcher.

CONTENTS

ABSTRACT 3
ACKNOWLEDGEMENTS 5
LIST OF TABLES 7
LIST OF FIGURES 7
LIST OF ABBREVIATIONS 88
1. INTRODUCTION 11
1.1. PXDN expression 11
1.2. Structure and function of PXDN 12
1.3. The role of PXDN in disease 15
1.3.1. Mutations in PXDN cause anterior segment dysgenesis 15
1.3.2. PXDN expression in cardiovascular disease 17
1.3.3. Peroxidasin dysregulation in cancer 18
1.4. Hypoxia-inducible factor-1 α 20
1.5. HIF-1α expression in cancer 22
1.6. Aims and Objectives 23
2. MATERIALS AND METHODS 23
2.1. Cell culture 23
2.2. Immunofluorescence confocal microscopy 24
2.3. Western blot 25
2.3.1. Cell lysis 25
2.3.2. Protein quantification 26
2.3.4. SDS-PAGE 26
2.3.5. Electrophoretic transfer and blocking 27
2.3.6. Antibody probing 28
2.3.7. Protein visualisation 28
2.4. Chromatin Immunoprecipitation 28
2.4.1. Bioinformatic analysis of the PXDN promoter 29
2.4.2. Primers design for PCR 29
2.4.3. Genomic DNA extraction 29
2.4.4. ChIP 30
2.4.5. PCR 31
3. RESULTS 32
4. DISCUSSION 38
REFERENCES 43

LIST OF TABLES

Table 2.1. SDS-PAGE polyacrylamide gel recipes 26
Table 2.2. Kapa Taq PCR reaction mix 31
Table 2.3. Kapa Taq cycling conditions 31
Table 2.4. ChIP PCR primer pairs 31

LIST OF FIGURES

Figure 1.1. Diagram showing the domains found in PXDN 14
Figure 1.2. PXDN catalyses the formation of collagen IV crosslinks …… 15
Figure 2.1. Electrophoresis transfer sandwich setup (Bio-Rad) ……..... 28
Figure 3.1. $CoCl_2$ treatment increases the protein expression of HIF-1α and LDHA 34
Figure 3.2. PXDN protein localises to the ECM of HeLa cells upon treatment with $CoCl_2$ ……..... 35
Figure 3.3 HIF-1α localises to the nucleus when the proteins expression is induced by treatment with $CoCl_2$ ……..... 36
Figure 3.4. LDHA expression increases in HeLa cells after 24h treatment with $CoCl_2$ 36
Figure 3.5. Bioinformatic analysis to determine putative HRE sites in the *pxdn* promoter region …..... 40
Figure 3.6. The pxdn promoter region contains an HRE that is bound by HIF-1 …..... 41

LIST OF ABBREVIATIONS

ALDO A – Aldolase A

Ang-II - Angiotensin II

APS - Ammonium persulphate

ARE - Antioxidant response element

ASD - Anterior segment dysgenesis ATP - Adenosine triphosphate

BSA - Bovine serum albumin

CBP - CREB-binding protein

ChIP - Chromatin immunoprecipitation

$CoCl_2$ - Cobalt chloride (II)

DAPI - 4',6-diamidino-2-phenylindole dihydrochloride

dH_2O - Distilled water

DMEM - Dulbecco's Modified Eagle's Medium

DUOX - Dual oxidases

ECM - Extracellular matrix

EDTA - Ethylenediaminetetraacetic acid

EMT - Epithelial mesenchymal transition

ENO1 – Enolase 1

EPO - Eosinophil peroxidase

ER - Endoplasmic reticulum

ERK - Extracellular-signal related kinase

FBS - Foetal bovine serum

FIH-1 - Factor inhibiting HIF-1

FIT C - Fluorescein isothiocyanate

H_2O_2 - Hydrogen peroxide

HEK293 - Human embryonic kidney cells 293

HIF-1α - Hypoxia inducible factor-1 alpha

HOBr - Hypobromous acid

HOCl - Hypochlorous acid

HRE - Hypoxia response element

HUVEC - Human umbilical vein endothelial cell

Ig - Immunoglobin

kDa - Kilodaltons

LDHA - Lactose dehydrogenase A

LDL - Low-density lipoproteins

LPO - Lactoperoxidase

LPS - Lipopolysaccharide

LRR - Leucine rich repeats

MG50 - Melanoma-associated Gene 50

MMP - Metalloproteinase

MPO - Myeloperoxidase

NOX - NADPH oxidase

Nrf2 - Nuclear factor erythroid 2-related factor 2

PBS - Phosphate buffered saline

PCR - Polymerase chain reaction

PHD - Prolyl hydroxylases

PRG2 - p53 response gene 2

PXDN - Peroxidasin

RIPA - Radio immunoprecipitation buffer

ROS - Reactive oxygen species

SDS - Sodium dodecyl sulphate

SDS-PAGE - Sodium dodecyl sulphate-polyacrylamide gel electrophoresis

SFN - Sulforaphane

tBHQ - *tert*-Butlyhydroquinone

TBS/T - Tris buffered saline/Tween

TCA - Trichloroacetic acid

TEMED - Tetramethylenediamine

TGF-β1 - Transforming growth factor- β1

TNF-α - Tumour necrosis factor-α

TPO - Thyroid peroxidase

vHL - von Hippel Lindau

VPO1 - Vascular Peroxidase 1

vWF - von Willebrand Factor

1. INTRODUCTION

Peroxidases catalyse the oxidation of various substrates in the presence of hydrogen peroxide (H_2O_2) resulting in the production of either organic radicals or inorganic hypohalous acids (Battistuzzi, *et al*, 2010). Depending on their sequence similarity, they can be grouped into two superfamilies: the first comprises all peroxidases in bacteria, fungi and plants, whereas vertebrate peroxidases are part of the peroxidase-cyclooxygenase superfamily (Battistuzzi, *et al*, 2010; Zamocky *et al*, 2008). In mammals, there are five known haem-peroxidases, namely myeloperoxidase (MPO), eosinophil peroxidase (EPO), lactoperoxidase (LPO) – which act in host defence through their antimicrobial activity, thyroid peroxidase (TPO) – a catalyst for thyroid hormone production and peroxidasin (PXDN) – a protein essential for basement membrane consolidation (Nelson *et al*, 1994; Cheng *et al*, 2008). PXDN is the most recently characterised haem-peroxidase and multiple studies have been carried out to elucidate its structure, function and role in pathophysiology. Here we investigate the regulation of *pxdn* in response to cellular hypoxia.

1.1. PXDN expression

The PXDN protein was identified and characterised as a haem-peroxidase with additional domains characteristic of extracellular interacting proteins in Drosophila (Nelson *et al*, 1994). During Drosophila development, PXDN is secreted by haemocytes into the extracellular matrix (ECM) where it plays a role in basement membrane consolidation (Nelson *et al*, 1994). The protein is also expressed in Drosophila phagosomes, oocytes, larval fat bodies and the gastric ceaca (Nelson *et al*, 1994). In *C. elegans*, PXDN is expressed in epidermal cells during embryogenesis where its role in basement membrane formation is vital for embryonic morphogenesis, muscle-epidermis attachment and neuronal guidance (Gotenstein *et al*, 2010). In addition to this, PXDN acts in the maintenance of cell adhesion in *C. elegans* in postembryonic tissue, and in the adult life stage PXDN is responsible for the inhibition of axon

regeneration (Gotenstein *et al*, 2010). *Xenopus tropicalis* was the first vertebrate wherein PXDN expression was observed (Tindall *et al*, 2005). Expression of PXDN in *X. tropicalis* was seen in the neural tube, optic vesicle, pronephros and tail-forming region during development and morphogenesis, where the protein is involved in modifying the ECM (Tindall *et al*, 2005). Regarding higher organisms, PXDN mRNA has been found to be expressed in the mouse during the embryonic stages of development, however the expression of the protein is found in the heart (Cheng *et al*, 2008). During development, the protein is expressed in the mouse corneal epithelium (Khan *et al*, 2011). In adult murine eyes the protein localises to the corneal and lens epithelium (Khan *et al*, 2011)

In humans, PXDN mRNA expression is widespread, with transcripts found in the heart, skeletal muscle, colon, spleen, kidney, liver, small intestine, lung, pancreatic and placental tissues (Pertefi *et al*, 2009). However, PXDN protein expression varies significantly from mRNA expression, with high expression of the protein seen primarily in the cardiovascular system (as such the protein is also known as vascular peroxidase-1 (VPO1)) where the protein is constitutively secreted by vascular endothelial cells and micromolar concentrations of the protein circulate in the bloodstream (Cheng *et al*, 2008; Cheng *et al*, 2011). In terms of cellular localisation, Pertefi *et al* reported that in human primary fibroblasts, human dermal fibroblasts, vascular endothelial cells and smooth muscle cells, PXDN localises to the endoplasmic reticulum (ER) (Pertefi *et al*, 2009). However, Cheng *et al* found that heterologously expressed PXDN was rapidly secreted into the culture medium of HEK293 cells with little protein found in cell lysates (Cheng *et al*, 2011).

PXDN expression may be induced or altered in response various stimuli such as transforming growth factor-β1 (TGF-β1), tumour necrosis factor-α (TNF-α), lipopolysaccaride (LPS), H_2O_2, and angiotensin-II (Ang-II) (Pertefi *et al*, 2009; Cheng *et al*, 2011; Hanmer and Mavri-Damelin, 2018; Shi *et al*, 2010). Upon stimulation with TGF-β1, human primary fibroblasts, human dermal fibroblasts, vascular endothelial cells and smooth muscle cells secrete PXDN into the ECM where the protein then localises to fibril-like structures (Pertefi

et al, 2009). In the cancer cell lines SiHa and HeLa however, TGF-β1 treatment caused a significant decrease in PXDN expression (Sitole and Mavri-Damelin, 2018). The proinflammatory factors tumour necrosis factor-α (TNF-α) and lipopolysaccharide (LPS) increased both *pxdn* transcription and PXDN expression in HUVECs (a vascular endothelial cell line) (Cheng *et al*, 2011). Treatment of HEK293 and HeLa cells with H_2O_2 resulted in increased PXDN expression (Hanmer and Mavri-Damelin, 2018). LPS was found to increase PXDN expression by approximately 4-fold (Shi *et al*, 2018). Angiotensin II (AngII) mediates the proliferation of vascular smooth muscle cells by upregulating PXDN expression (Shi *et al*, 2010).

1.2. Structure and function of PXDN

The human *pxdn* gene is found on chromosome 2p25, with an exon count of 24 and encodes a 165 kilodaltons (kDa) multidomain protein (NM_012293.3; NP_036425.1) (Geer *et al*, 2010; O'Leary *et al*, 2016). Although Nelson *et al* reported that the Drosophila homolog of PXDN exists as a trimer, the quaternary structure of mammalian PXDN is not clear (Nelson *et al*, 1994). Cheng *et al* describe human PXDN as a monomeric polypeptide (Cheng *et al*, 2011). However, contrary to this, Lazar *et al* observed that heterogously and endogenously expressed PXDN produced three separate band sizes (160kDa, 300kDa and 500kDa) of which the 500kDa was the most abundant (Lazar *et al*, 2015). They thus concluded that mammalian PXDN formed oligomers and that its dominant form was trimeric (Lazar *et al*, 2015).

Typically, mammalian haem-peroxidases contain an N-terminal signal peptide and a peroxidase domain. In addition to this, PXDN also contains five leucine rich repeats (LRR) with capping motifs, four immunoglobin (Ig) -binding domains and a C-terminal von Willebrand factor (vWF) (*Figure 1.1*.) (Cheng *et al*, 2008; Soudi *et al*, 2012). LRR are found in many proteins where they function in cell adhesion, signal transduction, ECM assembly, immune response and various other protein protein interactions (Kobe and Diesenhofer, 1995). The C-type Ig domain in PXDN commonly functions in cell adhesion and pattern recognition (Soudi *et al*, 2012). The domain is required, alongside

the catalytic peroxidase domain, for sulfilimine cross-link formations in collagen IV (Ero-Trolliver *et al*, 2015). It has been proposed that the N-terminal portion of this domain transiently interacts with collagen IV, allowing the hypobromous acid produced by the PXDN peroxidase domain interaction with the collagen NC1 substrate, facilitating crosslink formation (Ero-Trolliver *et al*, 2015). The loss of an N-terminal portion of this domain resulted in poor cross-linking between collagen IV molecules (Ero-Trolliver *et al*, 2015). The C-terminal vWF domain is the most recently characterised motif in peroxidases (Cheng *et al*, 2008). Proprotein convertase processing enhances PXDNs ability to crosslink collagen IV in the basement membrane (Colon and Bhave, 2016). PXDN is cleaved at the C-terminal preceding the vWF domain to activate PXDN catalytic activity (Colon and Bhave, 2016). In the absence of the proprotein convertase proteolytic processing, PXDN is still able to catalyse collagen IV however, its catalytic activity is significantly reduced (Colon and Bhave, 2016).

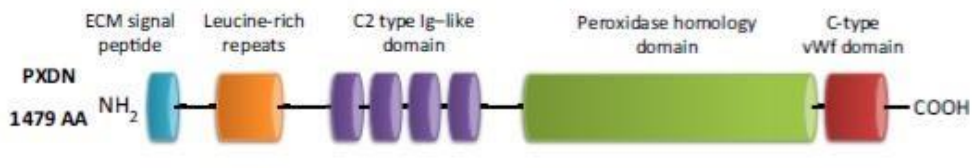

Figure 1.1. Diagram showing the domains found in PXDN. *In addition to its peroxidase domain, PXDN contains six LRR motifs, four Ig-like domains and a C-terminal vWF domain. These additional structures are thought to mediate interactions between PXDN and ECM proteins. (Peterfi and Geiszt, 2014).*

The haem-peroxidase domain of PXDN facilitates the formation of sulfilimine bonds in collagen IV through its production of hypohalous acids using H_2O_2 (Bhave *et al*, 2012; Lazar *et al*, 2015; Bathish *et al*, 2018). The source of H_2O_2 used in this reaction is yet to be established. Initially, Liu *et al* proposed NOX4 as the source of H_2O_2 for PXDN during inflammatory reaction in a model of pulmonary hypertension (Liu *et al*, 2014). This seemed to be corroborated by the 100-fold increase in NOX4 expression seen by Peterfi *et al* in myofibroblasts; however, it has been shown that PXDN promotes collagen IV

crosslinking in the absence of the NOX/DUOX families (Peterfi *et al*, 2009; Sirokmany *et al*, 2018). Still, it has been made clear that PXDN utilises this H_2O_2 to produce hypobromous acid which then oxidises methionine-93, which is cross-linked to lysine/hydroxylysine-211 at the non-collagenous interface of an adjoining collagen IV fibre (Bhave *et al*, 2012; Fidler *et al*, 2014; Ero-Tolliver *et al*, 2015; Bathish *et al*, 2018). Collagen IV fibres are the predominant fibres in the basement membrane protein network; therefore, this crosslinking reaction is important for maintaining basement membrane integrity (Bhave *et al*, 2012; Fidler *et al*, 2014; Lazar *et al*, 2015). The loss of peroxidase activity in Drosophilla and *C. elegans* results in poor basement membrane integrity and abnormal epidermal morphology, showing that PXDN sulfilimine bond formation is a key driver of basement membrane stability (Nelson *et al*, 1994; Gotenstein *et al*, 2010).

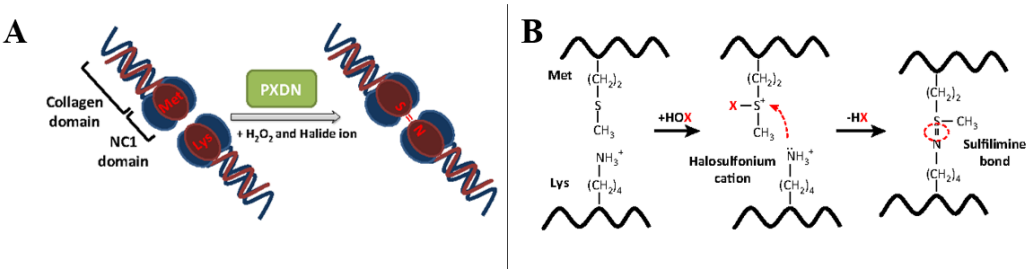

Figure 1.2. PXDN catalyses the formation of collagen IV crosslinks. *(A) Collagen IV crosslinks are formed at the NC1 interface of adjacent collagen fibres in the presence of PXDN, which catalyses the formation of hypohalous acid from H_2O_2. (B) Sulfilimine bonds are formed between opposing methionine and hydroxylysine residues using the hypohalous acid produced by PXDN as an intermediate (Peterfi and Geiszt, 2014).*

In addition to its role in ECM consolidation, it has been suggested that PXDN may play a role in innate immunity. Studies have shown that PXDN in plasma was able to effectively bind and kill *E. coli* through its production of HOCl, suggesting that PXDN plays a role in innate immunity in plasma (Li *et al*, 2012). The protein has also been found to mediate lung host defence through its ability to bind and kill gram-negative bacteria (Shi *et al*, 2018). The hypohalous acid generated by PXDN is bacteriacidal against *P. aeruginosa*

and *E. coli*, which interact with the PXDN N terminal via their cell wall LPS (Shi *et al*, 2018).

Another essential role of PXDN is the catalysis of dityrosine crosslinking reactions. In Drosophila, these stabilised the chorionic membrane and promoted ECM consolidation, however, it is thought that the dityrosine crosslinking reactions catalysed by PXDN may only occur under basic conditions (Nelson *et al*, 1994; Cheng *et al*, 2011).

1.3. The role of PXDN in disease

Oxidative stress refers to a disruption in redox balance within the cellular environment that leads to the production of excess ROS in the form of free radicals (O_2^- and OH^-), H_2O_2 and hypohalous acids. This preference for the pro-oxidative state leads to increased DNA damage, changes in protein function due to their oxidation and the peroxidation of cellular lipids. PXDN can act as a mediator of oxidative stress through the production of HOCl and HOBr, leading to cellular damage that results in disease. For example, in murine eye development, a nonsense mutation in the *pxdn* gene result in the loss of peroxidase activity, resulting in increased ocular inflammation (Yan *et al*, 2014). In cardiovascular disease for example, changes in PXDN expression lead to excessive HOCl formation that leads to endothelial cell damage. In this section, PXDN pathophysiology and its role in the development various disease will be discussed.

1.3.1. Mutations in PXDN cause anterior segment dysgenesis

PXDN is expressed during eye development in *X. tropicalis*, mice and humans (Tindall *et al*, 2005; Khan *et al*, 2012; Yan *et al*, 2014; Choi *et al*, 2014). Homozygous mutations in *pxdn* have been correlated with anterior segment dysgenesis (ASD) (a collection of developmental disorders affecting the anterior chamber of the eye), glaucoma and micropthalmia (Khan *et al*, 2012; Yan *et al*, 2014; Choi *et al*, 2015). Khan *et al* first described the presence of congenital eye defects in 5 families that carried mutations in *pxdn* (Khan *et al*,

2011). Later on, Choi *et al* identified four mutations that caused ASD – a maternally inherited nonsense mutation, a paternally inherited deletion that caused a frameshift mutation resulting in premature protein truncation, a maternally inherited frameshift mutation and a paternal deleterious missense substitution (Choi *et al*, 2015). What is yet to be described is how each mutation affects ocular development and whether each mutation differs in the phenotypic presentation of ASD. In a murine model, a nonsense mutation in *pxdn* resulted in the insertion of a premature stop codon (Yan *et al*, 2014). This mutation resulted in the loss of the peroxidase activity and the vWF domain (Yan *et al*, 2014). PXDN expression is responsible for the development of corneal and lens epithelium during eye development (Khan *et al*, 2011). In these structures, PXDN may be necessary for adhesive support and oxidative balance (Khan *et al*, 2011). The absence of PXDN expression in these cells results in the varying degrees of ASD which includes corneal opacity, cataract formation, micropthalmia and glaucoma (Khan *et al*, 2011; Yan *et al*, 2014; Choi *et al*, 2015). The reduced eye size seen in *pxdn* mutants is due to the decreased proliferation and differentiation of the lens (Yan *et al*, 2014). However, cataract formation, corneal opacity and glaucoma may occur as a result of aberrant oxidative balance in the developing eye. The absence of PXDN in the eye may result in the build-up of H_2O_2, resulting in protein and lipid oxidation leading to the deposition of the insoluble aggregates characteristic of cataracts and corneal opacification (Khan *et al*, 2011). Yan *et al* (2014) reported increased IL-β and TNF-α factors in mice carrying a *pxdn* mutation. The presence of these pro-inflammatory factors and increased ROS may be reason for the development of glaucoma.

Mice that carried the PXDN mutant gene suffered from severe anterior segment dysgenesis and microphthalmia (Yan *et al*, 2014). The mice also show decreased lens fibre cell proliferation and differentiation during development, which was the cause for decreased eye size (Yan *et al*, 2014). The loss of PXDN leads to decreased structural integrity in the lens epithelium, as the crosslinking of collagen IV is disrupted; indeed, collagen IV was decreased in the lens capsule and lens epithelium of mice carrying *pxdn* mutations (Yan *et al*, 2014). The loss of PXDN also leads to increased ocular

inflammation and glaucoma, which was noted through the increased expression of the inflammatory factors IL-1β and TNF-α (Yan *et al*, 2014). The authors hypothesise that this may be due to the loss of PXDN's peroxidase activity, which may mitigate the effects of increased ROS in the lens epithelium (Khan *et al*, 2011; Yan *et al*, 2014).

1.3.2. PXDN expression in cardiovascular disease

Atherosclerosis refers to the narrowing of blood vessels due to the formation of cholesterol or calcified plaques along the vessel walls (Kher and Marsh, 2004). PXDN interacts with and oxidises LDL through the HOCl generated by its peroxidase activity (Yang *et al*, 2016). This process results in a positive feedback loop as the presence of ox-LDL and LDL further increase PXDN mRNA and protein expression in human vascular endothelial cells (HUVECs), the human monocytic-like THP-1 cell line and mouse aorta (Bai *et al*, 2011; Yang *et al*, 2016). Furthermore, PXDN promotes the accumulation of lipid in macrophages (Yang et al, 2016). This is a result of its ability to bind and oxidise LDL; however, PXDN also oxidises the apoE protein responsible for binding very low-density lipoproteins (VLDL), thus impairing lipid clearance in the plasma (Yang *et al*, 2013). In addition to this, increased PXDN resulted in ox-LDL induced apoptosis via the caspase 3 pathway (Bai *et al*, 2011). Although the direct interaction of PXDN and caspase 3 are not shown, the inhibition of PXDN resulted in decreased endothelial cell apoptosis and reduced caspase 3 activity (Bai *et al*, 2011). In vascular smooth muscle cells (VSMCs), the increased PXDN expression leads to mineral deposition in endothelial cells (Tang *et al*, 2015). The activation of VPO1 in VSMCs correlated with the increased expression of the Runx2, an osteogenic transcription factor responsible for the endogenous regulation of vascular calcification (Tang *et al*, 2015). Vascular calcification is a precursor for the development of atherosclerosis disease, as well as diabetes and chronic kidney disease. The build-up of plaque is accompanied by a proinflammatory response that results in the formation of foam cells within the vasculature. As

previously mentioned, LPS and TNF-α induce PXDN expression and secretion in vascular endothelial cells (Cheng *et al*, 2011). In mouse aortic walls, the pro-inflammatory factors LPS and TNF-α result in the induction and accumulation of PXDN and ox-LDL (Yang *et al*, 2016). This chronic inflammatory response is responsible for the conversion of macrophages and endothelial cells into lipid-filled foam cells (Chistiakov *et al*, 2017).

PXDN regulates cardiac fibrosis after myocardial infarction (Liu *et al*, 2019). In human and murine hearts, following myocardial infarction, an increased PXDN expression leads to the differentiation of cardiac fibroblasts into myofibroblasts that are able to proliferate and deposit excess collagen I in the ECM leading to the progression of fibrosis (Liu *et al*, 2019). Furthermore, PXDN was co-expressed with α-SMA – a myofibroblast marker only expressed in hypertrophic and fibrotic hearts (Campbell and Katwa, 1997). Nonetheless, this function of PXDN in cardiac fibrosis simply emphasizes the role of the protein in vascular remodelling. In cardiovascular disease, vascular remodelling occurs as an adaptive response to changes in pressure, ischemia and multiple other injuries. In spontaneously hypertensive rats, PXDN expression is increased alongside MMP-2 and MMP-9 resulting in the degradation and reorganization of the ECM that leads to increased blood pressure (Iiangqing *et al*, 2017).

1.3.3. Peroxidasin dysregulation in cancer

PXDN dysregulation has been associated with at least four cancer hallmarks (proliferation, apoptosis, angiogenesis, metastasis and invasion) in breast, colon and ovarian cancers, as well as melanoma, renal cell carcinoma, glioblastomas, prostate cancer, cervical cancer and ovarian cancer (Mitchell *et al*, 2000; Jayachandran *et al*, 2016; Castranova *et al*, 2006; Tauber *et al*, 2010; Barnett *et al*, 2010; Liu *et al*, 2010; Woods, 2013; Sitole and Mavri-Damelin, 2018; Hanmer and Mavri-Damelin, 2018; Zheng and Liang, 2018). In these malignant cancers, two processes remain key constituents of their progression; that is the increased production of ROS, which leads to the redox imbalance that facilitates progression, angiogenesis and survival, as well as EMT which

enables the invasive and metastatic characteristics of tumours. PXDN has been strongly associated with both the process of ROS production and EMT in cancer.

High levels of ROS are known to be a key driver of cancer survival. PXDN produces ROS through the catalysis of H_2O_2 to HOBr – a process key to basement membrane synthesis and innate immunity. However, in cancer PXDN dysregulation may cause increased ROS leading to apoptosis and EMT. In the EB1 colon cancer cell line, PXDN (p53-response gene 2 or PRG2) was identified as a response gene upregulated during the process of p53-dependant apoptosis (Horikoshi *et al*, 1999). In these EB1 cells, a 4.5kb mRNA transcript of PXDN was found (Horikoshi et al, 1999) The shorter transcript encoded the portion of PXDN that carried the peroxidase domain without the N terminal signal peptide, which left room for the hypothesis that during p53 mediated apoptosis, PXDN accumulated in the cells and increased cellular ROS, leading to the activation of caspases and other downstream players responsible for apoptosis (Horikoshi et al, 1999).

More recently, it has been shown that Nrf2, the master regulator of redox response, binds the PXDN promoter and activates transcription of the gene (Hanmer and Mavri-Damelin, 2018). This work showed that both PXDN and Nrf2 protein expression increased in the presence of H_2O_2, and the expression of both proteins was further upregulated when cervical cancer cell lines were treated with SFN and tBHQ – known inducers of Nrf2 expression. Furthermore, treatment with H_2O_2 resulted in the perinuclear expression of PXDN, whereas upon treatment with SFN and tBHQ, PXDN was deposited in the ECM. ChIP and luciferase assay then confirmed that the PXDN promoter contains an antioxidant response element (ARE) that is bound by Nrf2 during oxidative stress resulting in increased expression and secretion of the PXDN gene (Hanmer and Mavri-Damelin, 2018). Although the expression of PXDN through activation by Nrf2 is increased in cervical cancer cells, PXDN expression is also significantly increased in the embryonic cell line HEK293 (Hanmer and Mavri-Damelin, 2018). This could reflect the nature of PXDN which is expressed during development, however this may also reflect the

ability of Nrf2 to mitigate the effects of oxidative stress in normal cells, whilst still being able to drive cancer progression in tumours. Nonetheless, these results reveal that PXDN is directly implicated in cancer progression through changes in redox regulation.

The direct association between PXDN and oxidative stress through its activation by Nrf2, broadens the implications for PXDN expression in cancer cells. ROS is known to be a secondary cellular messenger that directs a variety of biological processes in cancer (Janssen-Heininger *et al*, 2008). Epithelial to mesenchymal transition (EMT) is one of those processes. ROS is able to regulate ECM remodelling, cytoskeleton remodelling, cell-cell junction and cell motility, leading to EMT and allowing for the invasion-metastasis cascade in the later stages of cancer progression (Ye and Weinberg, 2015). EMT is a process whereby epithelial cells associated with the basement membrane differentiate and take on a mesenchymal phenotype (Ye and Weinberg, 2015). These changes result in increased cell motility, allowing for the migration from the local tumour environment and colonisation of distant tissues.

PXDN expression was correlated with the expression of haem oxygenase-1 (HO-1) (Tauber *et al*, 2010). HO-1 is a key enzyme in haem degradation. In normal cells, HO-1 has cytoprotective, anti-inflammatory, antiproliferative and antiapoptotic roles, however in malignant cells the protein aids in cell survival, apoptosis, invasion and metastasis as well as drug resistance. The expression of the protein varies in response to certain stimuli, including ROS. In choriocarcinoma cells, HO-1 was strongly correlated with PXDN, where the proteins facilitated cell adhesion (Tauber *et al*, 2010). Increased cellular HO-1 resulted in increased adhesion to various ECM molecules in BeWo cells, and this increased expression of HO-1 correlated with an increased expression of PXDN (Tauber *et al*, 2010). Moreover, the loss of PXDN in the choriocarcinoma cell line resulted in the loss of adhesion in cells expressing HO-1 (Tauber *et al*, 2010).

PXDN has been closely associated with TGF-β1. In kidney fibrosis, PXDN is secreted to the ECM in response to TGF-β1 treatment, whereas in cervical

cancer, TGF-β1 causes decreased extracellular PXDN expression (Peterfi *et al*, 2009; Sitole and Mavri-Damelin, 2018). TGF-β1 regulates cell proliferation and cell adhesion, and the cytokine plays a role in EMT induction by the activation of Snai1, which then represses E-cadherin (Katsuno *et al*, 2013). ROS signalling is an important factor in this process as decreased ROS results in the reversal of TGF-β1 induced EMT (Katsuno *et al*, 2013). Once the TGF-β1 pathway is activated by ROS, a positive feedback loop causes the increased production of ROS by TGF-β1, leading to EMT progression (Katsuno *et al*, 2013). Moreover, ROS also causes increased Snai1 expression (Hanmer and Mavri-Damelin, 2018). In the cervical cancer cell lines HeLa and SiHa, TGF-β1 treatment resulted in a switch to a mesenchymal phenotype (Sitole and Mavri-Damelin, 2018). The PXDN expression in these cells had decreased significantly with E-cadherin, whereas the EMT markers, Snai1 and vimentin, were markedly increased (Sitole and Mavri-Damelin, 2018). In addition to this, ChIP and luciferase assay showed that Snai1 binds an E-box in the PXDN promoter region and represses PXDN expression (Sitole and Mavri-Damelin, 2018). Barnett *et al* (2010) identified PXDN as an oxidative response gene that whose mRNA expression was upregulated more than 300-fold in prostate cancer. The differences here may be attributed to stage- and tissue specific expression of the PXDN gene in tumour progression.

1.4. Hypoxia-inducible factor-1 α

The maintenance of O_2 homeostasis is vital for cellular functioning, thus decreased O_2 within the cell environment results in a signalling pathway cascade that aims to restore homeostasis (Vafhakha and Gilany, 2010). The hypoxia inducible factor-1 (HIF-1) transcription factor is the master regulator of multiple physiological processes in response to hypoxia (Semenza, 2001). The HIF-1 protein is a heterodimer whose two subunits consist of a basic helix-loop-helix (bHLH) and PAS domain, which is important for subunit dimerization and binding of the hypoxia response element (HRE) – a consensus 5′-ACGTG-3′ sequence in the promoter or enhancer region of

multiple genes *(Figure 1.3.)* (Semenza *et al*, 1992; Wang *et al*, 1995; Chapman-Smith *et al*, 2004; Yang *et al*, 2005; Dengler *et al*, 2014). The HIF-1 complex consists of a constitutively expressed HIF-1β subunit and an oxygen-dependant alpha subunit (Wang and Semenza, 1995; Wang *et al*, 1995). There are three known isoforms of the alpha subunit; namely HIF-1α, HIF-2α and HIF-3α. Little research has been conducted on HIF-3α, however HIF-1α and HIF-2α are both activated in response to hypoxia. HIF-1α plays a role in acute response (~2-24hrs) whereas HIF-2α is activated in response to chronic hypoxia (~48-72hrs) (Holmquist-Mengelbier *et al*, 2006; Koh *et al*, 2011; Koh and Powis, 2012). In addition to this, HIF-2α expression is activated when cellular O_2 is decreased to ~5%, whereas HIF-1α expression occurs during severe hypoxia (O_2<1%) (Holmquist-Mengelbier *et al*, 2006). Although both proteins are expressed during hypoxia, HIF-1α is of interest in this study because it acts as the master regulator ofof acute hypoxia –the physiological state that this work focuses on.

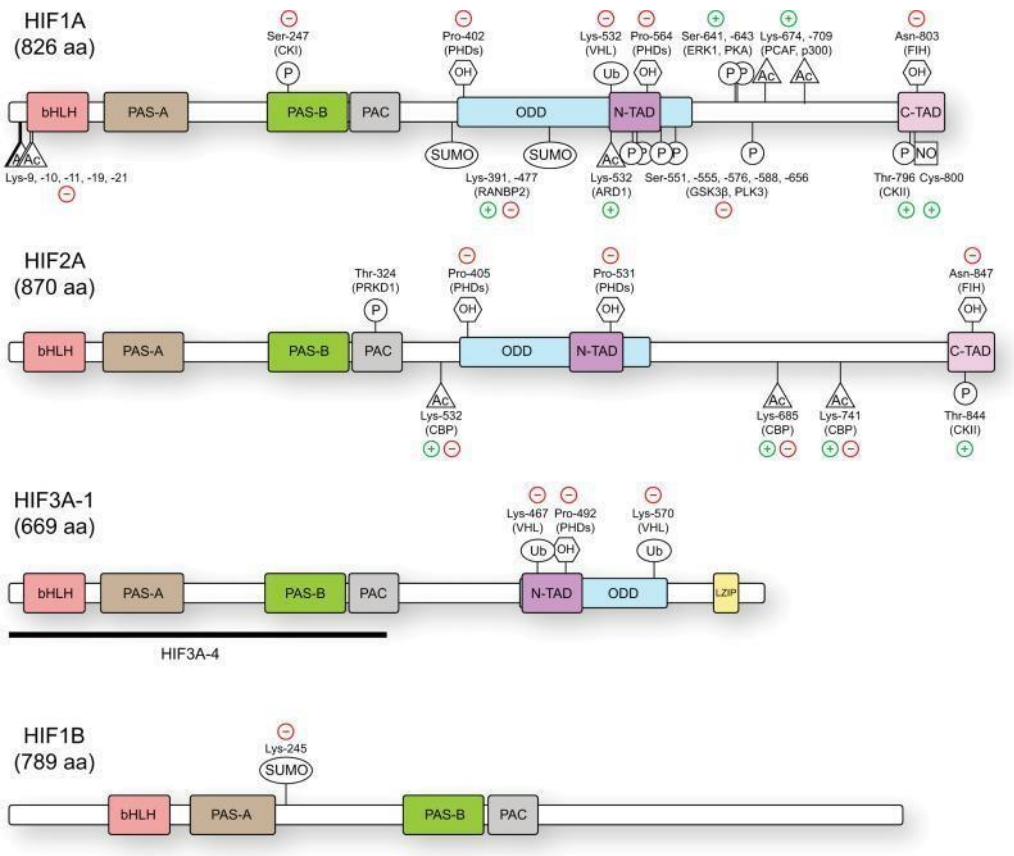

Figure 1.3. HIF domains and post-transcriptional modifications. *HIF proteins contain a number of conserved protein domains. The basic Helix Loop-Helix domain (bHLH) for DNA binding, dimerization through the PAS domains. The oxygen dependant domain (ODD) acts in oxygen sensing and transcriptional activation domains (N-TAD and C-TAD). HIF regulation and activation occurs through the structural modification of the various domains by amino acid residues (Dengler et al, 2014).*

The expression of the HIF-1α subunit is tightly regulated during normoxia. When cellular oxygen levels are within a normal range, post-translational modifications such as hydroxylation, acetylation and ubiquitination regulate HIF-1α in an oxygen dependant manner. HIF-1α is hydroxylated at P402 and P564 by the prolyl hydroxylase domain (PHD) protein in a 2-oxoglutarate and O_2-dependant reaction, requiring Fe^{2+} and ascorbate as co-factors (Salceda and Caro, 1997; Huang *et al*. 1998; Kallio *et al*, 1999). Factor Inhibiting HIF-1 (FIH-1) hydroxylates the A803 residue of the protein preventing the interaction of the transcriptional co-activator CREB-binding protein/p300 resulting in the repression of HIF-1 expression (Mahon *et al*, 2001). Furthermore, the acetyl transferase ARD-1 also acetylates the protein at K532. Collectively, these modifications lead to the interaction of HIF-1α with the von Hippel Lindau complex (pVHL), which targets HIF-1α by attaching polyubiquitin chains at L574 for proteasomal degradation (Wykoff *et al*, 20002000). This degradational process maintains the short half-life ($t_{½}$ = 5 minutes) of HIF-1α during normoxia (Ke and Costa, 2006).

During hypoxia, however, PHDs and FIH-1 are inactivated and HIF-1α expression is upregulated. HIF-1α is translocated from the cytoplasm into the nucleus where it interacts with the constitutively expressed HIF-1β, forming the HIF-1 complex (Kallio *et al*, 1998; Semenza 2000). The HIF-1 heterodimer is now transcriptionally active and binds the HRE in the promoter or enhancer region of multiple genes (Semenza, 2000). Approximately 2% of all genes involved in response to hypoxia are regulated by HIF-1, these include genes responsible for erythropoiesis, angiogenesis, glucose metabolism, iron homeostasis and proliferation. The activation of these pathways aims at decreasing cellular O_2 consumption and increasing O_2 delivery. For example,

the first HIF target gene identified was erythropoietin (EPO), a glycoprotein hormone that stimulates the generation of new red blood cells, thereby increasing O_2 delivery (Semenza and Wang, 1992).

1.5. HIF-1α expression in cancer

HIF-1α activation plays a crucial role in the adaptive response of tumour cells to changes in oxygen through its activation of genes involved in glucose metabolism, cell proliferation, migration and angiogenesis (Semenza, 2001). For example, HIF-1 facilitates the metabolic switch from oxidative phosphorylation to the glycolytic pathway to maintain the increasing glucose needs of the tumour within its continuously changing microenvironment (Semenza, 2001). This process is known as the Warburg effect (Weinhouse *et al*, 1956). HIF-1 mediates this process through the transcriptional activation of glycolytic enzymes and glucose transporters, which in turn increase the glucose levels within the tumour microenvironment (Denco, 2008). As tumour cells grow, decreased oxygen is available to the tumour therefore, HIF-1 responds to this hypoxic microenvironment by inducing the transcription of pro-angiogenic factors to maintain oxygen and nutrient supply of developing tumours (Conway *et al*, 2001). Once the tumour can no longer grow in its primary site, HIF-1 assists in the metastasis of tumour cells through the activation of transforming growth factor β3 and epidermal growth factor (EGF) – allowing the cells to adapt to the microenvironment in distant sites (Conway *et al*, 2001). Although the role of HIF-1 in cancer is more complex than described, these examples show that the HIF-1 protein plays a significant role in the development and progression of tumours.

1.6. Aims and Objectives

The aim of this research was to determine whether HIF-1α regulates *peroxidasin*.

To achieve this, the following objectives were carried out:

- Determination of the cellular localisation of PXDN and HIF-1α in response to chemically induced hypoxia using immunofluorescence confocal microscopy.
- Quantification of PXDN and HIF-1α protein expression in response to hypoxia using Western blot.
- The interactions between HIF-1α and the PXDN promoter region were observed using chromatin immunoprecipitation (ChIP) and PCR.

2. MATERIALS AND METHODS

2.1. Cell culture

The HeLa human cervical adenocarcinoma cell line (Cellonex) used for this study was cultured in Dulbecco's Modified Eagle's Medium (DMEM):Ham's F12 Nutrient Mixture (F12) (3:1 ratio), supplemented with 10% Fetal Bovine Serum (FBS) and 100 U/ml penicillin/0.1 mg/ml streptomycin. Cells were maintained at 37°C in a humidified 5% CO_2 atmosphere incubator. To maintain the cell line, medium was replaced as needed and sub-cultured once they reached 70-90% confluency. Cells were sub-cultured by rinsing cells three times with 1X phosphate buffered saline (PBS) before adding 500 µl Trypsin: EDTA diluted in 1.5 ml 1XPBS and incubated at 37°C for 3 minutes. After cells had detached, 500 µl of cell suspension was added to 9.5 ml of fresh culture medium.

For confocal microscopy, cells were seeded at a density of 150000 cells/well of a 6 well plate. The cell counting was done by mixing 10 µlµ of trypsinized cells with 10 µl of 0.2% w/v Trypan blue. Cells were counted using a haemocytometer, and the counts used to calculate the cell concentration and the volume of cells to be added to each well. After seeding cells were left to grow for 24 hrs before treatment.

All cell treatments were done using 100 µM $CoCl_2$ – a hypoxia mimetic that acts by binding the active site of the PHD that degrades HIF-1α, thus allowing for HIF-1α accumulation in the cells (Mahey *et al*, 2016). Cells were treated 24 hrs after seeding for either 3 hrs, 6 hrs, 12 hrs, or 24 hrs for immunofluorescence microscopy and Western blot; and for ChIP, cells were treated for 12hrs only.

2.2. Immunofluorescence confocal microscopy

Immunofluorescence microscopy was used to visualise the expression and cellular localisation of PXDN, HIF-1α and LDHA. Unless otherwise stated, all washes were done using 1XPBS for 5 minutes and each buffer was diluted in 1XPBS; all steps were carried out on a shaker. After seeding and treatment, cells were washed once with cold 1XPBS and fixed to coverslips for 15 minutes using 3% (v/v) formaldehyde. Cells were then washed 3 times and permeabilised for 1 hr with 0.25%(v/v) Triton X-100. The cells were washed another 3 times and coverslips blocked with 0.5%(w/v) BSA for 30 minutes. Cells were washed once more and incubated with primary antibodies (1:200), diluted in 0.5% (w/v) BSA overnight at 4°C. Following overnight incubation, cells were washed 3 times with 0.5%(w/v) BSA and incubated for 2 hrs in a dark chamber at room temperature with fluorescein isothiocyanate (FIT-C) conjugated goat anti-mouse IgG1 secondary antibody (Thermo Fischer Scientific, Waltham, Massachusetts, United States) (1:500) diluted in 0.5%(w/v) BSA. To prevent photobleaching, the remaining steps were carried out in the dark. After the 2-hr incubation, cells were washed 3 times and their nuclei counterstained with 0.1μg/ml 4', 6-diamidino-2-phenylindole dihydrochloride (DAPI) for 5 minutes. Finally, cells were washed 3 more times and coverslips then mounted onto a slide using Fluoromount Aqueous Mounting Medium. The slides were left to set for 2 hrs in the dark at room temperature, afterwards they were stored at 4°C in the dark until visualisation. Stained cells were visualised using a Carl Zeiss LSM 780 confocal microscope with Zen 2010 software. DAPI and FIT-C fluorophores were detected at 405/454 and 488/525 excitation/emission spectrums, respectively, using 63x magnification.

2.3. Western blot

Western blot was conducted to determine the expression levels of PXDN, HIF-1α and LDHA. β-actin was used as a loading control. Total protein was extracted from cells and quantified using the Bramhall assay (Bramhall *et al*, 1969). Proteins were then separated according to size using reducing sodium dodecyl sulphate polyacrylamide gel electrophoresis (SDS-PAGE) and a broad range pre-stained protein standard used for reference (New England BioLabs, Ipswich, Massachusetts, USA). Separated proteins contained in the gel were transferred onto a nitrocellulose membrane and the proteins of interest were probed for using specific antibodies. Protein bands were detected using chemiluminescence and signals captured on X-ray film for quantification.

2.3.1. Cell lysis

Cells were seeded into 10 cm dishes and treated overnight with 100 μM $CoCl_2$ for 3 hrs, 6 hrs, 12 hrs and 24 hrs. Once they had reached confluency, culture medium was aspirated from the cells, after which they were washed three times with cold 1XPBS. Cells were then scraped into a 1.5 ml microcentrifuge tube using 1ml 1XPBS and centrifuged at 11000 rpm for 10 minutes at 4°C. The 1XPBS was removed and 1X radioimmunoprecipitation assay (RIPA) buffer was added to the cells, they were vortexed briefly and then left on a rotator at 60 rpm at 4°C. Lysates were centrifuged at 12500 rpm for 5 minutes at 4°C and the supernatant containing the total cellular protein was aliquoted into PCR tubes and stored at -20°C. Total protein was quantified using the Bramhall assay (Bramhall *et al*, 1969).

2.3.2. Protein quantification

A grade 1 Whatman filter paper was soaked in distilled water (dH2O) for 20 minutes. After this, the filter paper was incubated, with shaking, in 95%(v/v) ethanol, 100% (v/v) ethanol and 100%(v/v) acetone for 5 minutes per solution. The filter paper was then allowed to dry. A standard curve was set up using a 1 mg/ml BSA stock solution with 1 µl, 3 µl, 6 µl, 12 µl, 16 µl and 20 µl being pipetted separately onto the filter paper, along with 2µl of each unknown sample. Protein samples were allowed to dry and the filter paper then soaked in 7.5%(v/v) trichloroacetic acid (TCA) for 45 minutes, with shaking. The filter paper was then soaked in Coomassie blue dye for 1hr to stain the proteins; after this the filter paper was incubated in destain solution for another hour. The filter paper was left to dry under a hood and then each standard and sample area was cut out and placed individually into 5ml of elution buffer overnight, in the dark. 160µl of each eluted sample was pipetted in triplicate into a well of a 96-well plate. Absorbance values were measured at 595nm using a Multiskan GO microplate reader (ThermoFisher Scientific). A standard curve of protein concentration (µg/µl) vs. absorbance (arbitrary units) was plotted using Microsoft Office Excel and unknown protein concentrations calculated using the equation of the standard curve (Bramhall *et al*, 1969).

2.3.4. SDS-PAGE

The Mini-PROTEAN® Tetra Cell system (Bio-Rad) was used for SDS-PAGE. Polyacrylamide gels was prepared according to the recipes provided in Table 2.1., and allowed to set within a glass plate sandwich. Either an 8% or 10% separating gel, for PXDN and HIF-1α or LDHA and β-actin respectively, with 5% stacking gel. Protein amounts quantified by Bramhall assay were prepared in a 3:1 ratio to 4X protein loading buffer (PLB) and boiled for 5 minutes to denature the proteins. Samples were then loaded onto the gel and the tank filled with SDS-PAGE running buffer. The gel was electrophoresed at a constant voltage of 180 V for approximately 1.5 hrs, depending on the size of the protein probed for.

Table 2.1. SDS-PAGE polyacrylamide gel recipes

	Separating gel (1 nl)		**Stacking gel (5ml)**
Reagent	**8%**	**10%**	**5%**
dH_2O	4.6ml	4ml	3.4ml
29:1 Bis acrylamide	2.7ml	3.3ml	830µl
1.5M Tris-HCl (pH8.8)	2.5ml	2.5ml	-
1M Tris-HCL (pH6.8)	-	-	630µl
10% (v/v) SDS	100µl	100µl	50µl
10% (v/v) APS	100µl	100µl	50µl
TEMED	6µl	5µl	4µl

2.3.5. Electrophoretic transfer and blocking

Following electrophoresis, the gel was removed and regions containing proteins of interest were cut out and placed into transfer buffer for 5 minutes in order to equilibrate. An electrophoresis sandwich (*Figure* 2.1.) was assembled for the transfer of proteins from the gel to nitrocellulose membranes and placed into BioRad Mini Trans-Blot® Electrophoretic Transfer Cell (Bio-Rad 170-3930) system filled with ice cold transfer buffer. Electrophoretic transfer was carried out at 4°C for 3 hrs at a constant 300 mA. Transfer buffer was changed hourly to maintain the cold temperature. Once the transfer was complete, the membranes were briefly rinsed in 1X Tris buffered saline/Tween-20 (TBS/T) and then placed into blocking buffer (5% (w/v) fat free milk or BSA) for 1-hr at room temperature with gentle shaking. After blocking, the nitrocellulose membranes were rinsed 3 times with cold 1XTBS/T for 5 minutes per wash.



Figure 2.1. Electrophoresis transfer sandwich setup (Bio-Rad). *The western blot transfer was setup using the Bio-Rad Mini Protean™ electrophoresis system. After SDS-PAGE, gel is placed alongside nitrocellulose membrane within a sandwich of filter paper. The electrophoresis sandwich is then placed in transfer buffer and a current that travels through the system transfers protein from the gel to the nitrocellulose membrane. Once this is complete the membrane may be probed for proteins of interest.*

2.3.6. Antibody probing

All antibodies used for this research were purchased from Santa Cruz Biotechnology, unless otherwise stated. Primary antibodies were diluted (1:1000) in either 5%(w/v) fat-free milk for LDHA or 5%(w/v) BSA for PXDN, HIF-1α and β-actin and incubated with corresponding nitrocellulose membranes overnight at 4°C with gentle agitation. Membranes were washed 3 times in cold 1XTBS/T for 5 minutes each and incubated with the m-IgGκ BP-HRP secondary antibody (1:2000), diluted in 5%(w/v) fat-free milk or BSA in 1XTBS/T for 1-hr at room temperature, in the dark, with gentle agitation. Nitrocellulose membranes were then washed another 5 times with cold 1XTBS/T. All antibodies used in these experiments were purchased from Santa Cruz Biotechnology (Dallas, Texas, USA).

2.3.7. Protein visualisation

The following procedure was carried out in a dark room. WesternBrightTM Chemiluminescent substrate produced by Advansta (San Jose, California, USA) was added to each nitrocellulose membrane and left for 5 minutes as the signal developed. Excess substrate was dabbed off onto Kimwipe and the nitrocellulose membranes were covered in plastic wrap. Bands were detected using X-ray film which was first exposed to the nitrocellulose membranes and then placed into developer solution, rinsed briefly in water and then placed into fixer solution. The films were rinsed in water once more and allowed to dry. The X-ray films were scanned and band intensity was quantified by densitometric analysis using Image Studio Lite (Ver. 5.2.) software.

2.4. Chromatin Immunoprecipitation

ChIP was performed to determine whether the HIF-1α protein binds the PXDN promoter region. This procedure involved crosslinking all bound proteins to DNA within cells, which were then sonicated to shear DNA into smaller fragments which could be used for PCR. The protein of interest was then immunoprecipitated from the sonicated sample using an anti-HIF-1α antibody. If the HIF-1 had bound a specific region of the PXDN promoter, the antibody would immunoprecipitate both the HIF-1 protein and promoter sequence it was crosslinked to. The DNA fragment could then be separated from the HIF-1 protein and amplified using PCR.

2.4.1. Bioinformatic analysis of the PXDN promoter

Since we identified that PXDN expression is modified by $CoCl_2$ we conducted a bioinformatic analysis of the PXDN promoter using JASPAR software to determine whether there were any putative HIF-1α binding sites in the PXDN promoter region (Khan *et al*, 2018). The first 1000bp upstream of the PXDN

translation start site were scanned for any putative HIF-1α binding sites and the consensus sequence was taken as 5'-ACGTG-3' (Semenza *et al*, 1992). We identified four putative HIF-1α binding sites upstream of the PXDN translation start site therefore primers for ChIP PCR were designed against all four regions of the PXDN promoter. A primer pair set covering a region of the promoter that did not contain any putative binding sites was included as a negative control.

2.4.2. Primers design for PCR

Primers were designed to amplify the two PXDN promoter regions: multiple pairs amplified across the putative HIF-1α binding sites that were identified by the bioinformatic analysis (PXDNHIF-1α+), and a single pair across the region without any HIF-1α binding sites (PXDNHIF-1α-). The LDHA promoter was used as a positive control and two primer sets were also used: one pair amplified across the known LDHA HRE site (LDHAHIF-1α+) and the other pair covered a region in the LDHA promoter that lacked an HRE (LDHAHIF-1α-) (Luo *et al*, 2011; Qui *et al*, 2014).

2.4.3. Genomic DNA extraction

In order to first test and optimise the annealing temperatures of the ChIP PCR primers (Table 2.4.), genomic DNA was extracted using the Quick g-DNA Miniprep Kit (Zymo Research – California, USA). Cells were cultured in 10 cm dishes, washed three times with 1XPBS, then scraped into 1 ml of 1XPBS. Cells were then centrifuged at 5000 rpm for 5 minutes at 4°C. Afterwards, the pellet was resuspended in genomic lysis buffer and left to stand for 5-10 minutes at room temperature. The mixture was then transferred into a Zymo-Spin IIC column in a collection tube and then centrifuged at 13500 rpm for 1 minute. The collection tube and flow through were discarded. The column was transferred into a new collection tube and DNA prewash buffer added to the spin column. The column was centrifuged again for 1 minute at 13500 rpm. g-

DNA wash buffer was added to the column and the column centrifuged once more for 1 minute at 13500 rpm. The spin column was then transferred to a 1.5 ml microcentrifuge tube and eluted in 10 mM Tris-HCl pH7.8. The eluted DNA was quantified on a NanoDrop ND-1000 Spectrophotometer at 260 nm and 280 nm, and stored at 20°C.

2.4.4. ChIP

HeLa cells were seeded into 10 cm dishes until 70% confluent then treated with 100 µM $CoCl_2$ for 12 hrs. Proteins bound to DNA were crosslinked using 1% (v/v) formaldehyde in fresh culture medium for 10 minutes with shaking, followed by the addition of 125 mM glycine for 5 minutes to quench the crosslinking reaction. Cells were washed 3 times with 1XPBS, scraped into a microcentrifuge tube and collected at 5000 rpm for 5 minutes at 4°C. Cells were then resuspended in 1XPBS and sonicated for 5 minutes at 40% amplitude on a 15s ON/OFF cycle using the Q125 Sonicator (QSonica – New York, USA). Cell debris was separated out by centrifugation at 10000 rpm for 10 minutes at 4°C. Sonicated DNA was resolved on a 1.5%(w/v) agarose gel, as described previously, in order to ensure the DNA fragments were the correct size (500-1000 bp) for downstream PCR. ChIP was performed on 15 µg of the sonicated lysate, diluted 1:10 in ChIP IP buffer, to which 4 µl of the mouse anti-HIF-1α antibody was added, and incubated at 4°C for 4 hrs while rotating at 10 rpm. 20 µl of Protein A/G agarose beads were added to each sample – a control containing band no antibody was included. The samples were then left rotating at 10 rpm overnight at 4°C. The following day, samples were washed. This included centrifugation at 5000 rpm for 1 minute followed by resuspension and rotation in wash buffer at 25 rpm for 5 minutes. This was repeated 3 times, and then once more using final wash buffer. DNA/protein crosslinks were reversed by adding ChIP elution buffer to each sample and then incubation in a water bath set at 65°C for 1-hr. The supernatant containing DNA/protein crosslinks was separated from the beads by centrifugation at 5000 rpm for 1 minute. DNA within the supernatant was purified with the

DNA Clean&Concentrator kit (Zymo Research – California, USA) and eluted in 50 µl 10 mM Tris-HCl pH7.8. Purified DNA was immediately used in ChIP PCR.

2.4.5. PCR

To amplify the binding site precipitated by ChIP, PCR was carried out using KAPA Taq ReadyMix (Merck KGaA – Darmstadt, Germany) was used for the ChIP PCR. A 25 µl reaction mix was setup as in Table 2.2. for each primer pair. The PCR was then run according to the cycling conditions in Table 2.3. using the annealing temperatures in Table 2.4. The reaction was run using the Applied Biosystems 2720 Thermal Cycler (Applied Biosystems South Africa – Fairland, Johannesburg). PCR products were then resolved on 1.5% (w/v) agarose gels. Agarose gels were visualised using the Bio-Rad Gel Doc XR (Biorad Laboratories – Rosebank, South Africa).

Table 2.2. Kapa Taq PCR reaction mix

Reagent	**Volume (µl)**
Kapa Taq Master Mix	12
Forward Primer	0.6
Reverse Primer	0.6
Template DNA	5
Nuclease free water	6.3
Total volume	25

Table 2.3. Kapa Taq cycling conditions

Step	Temperature (°C)	Duration	Cycles
Initial denaturation	95	3 minutes	1
Denaturation	95	30 seconds	1
Annealing	T_m-5	30 seconds	35
Extension	72	1 minute	
Final extension	72	1 minute	
Hold	4	∞	1

Table 2.4. Annealing temperatures for the ChIP PCR primer pairs

Primer pair	Primer sequence	Annealing temperature (°C)	Amplicon size (bp)
$PXDN_{HIF\text{-}1\alpha+}$ 1	F: 5′-CTGAATCTGGCACCGTCACCCTG-3′ R: 5′-AAAGCCCCTCATTCCTTTTGAGGA-3′	56.4	476
$PXDN_{HIF\text{-}1\alpha+}$ 2	F: 5′-CAGACTCCCTTGCTGTGCGCTTTG-3′ R: 5′-AGCTGTGCACATGCGCGCGAGGCT-3′	58	471
$PXDN_{HIF\text{-}1\alpha+}$ 3	F: 5′-GAACGTTAAATAATTTCCTACGT-3′ R: 5′-GGCGCAGAACAGCACGAGCG-3′	50	372
$PXDN_{HIF\text{-}1\alpha-}$	F: TTCTGTGTTGTACTCTCATTCTCT R: CAAGGACCCAGTCTGAATTTCACA	50	441
$LDHA_{HIF\text{-}1\alpha+}$	F: 5′-TTGGAGGGCAGCACCTTACTTAGA-3′ R: 5′-GCCTTAAGTGGAACAGCTATGCTGAC-3′	55	197
$LDHA_{HIF\text{-}1\alpha-}$	F: 5′-TTGAGTAGGATCCGCCGGTA-3′ R: 5′-AGCCGGGTCTCTCCTTACAA-3′	55	326

3. RESULTS

The aim of this research was to determine whether HIF-1 associates with the *pxdn* promoter region, thus being a putative regulator of the gene. Our first objective was to determine the expression and localisation of HIF-1α, PXDN and LDHA using immunofluorescence confocal microscopy. HeLa cells were treated with 100 μM $CoCl_2$ for 3 hrs, 6 hrs, 12 hrs and 24 hrs, afterwards they were each labelled with the corresponding anti-HIF-1α, anti-PXDN and anti-LDHA primary antibodies. The bound primary antibody was then targeted using a FIT-C-conjugated secondary antibody, and the nuclei counterstained with DAPI.

Figure 3.1. shows that the fluorescence for HIF-1α is increased in HeLa cells after 3 hrs of 100 μM $CoCl_2$ treatment. The protein ultimately localises to the nucleus as can be seen in the 24-hr panel of Figure 3.1. For PXDN (*Figure 3.2.*), fluorescence was seen in the untreated sample, however as the time for treatment increased, there was a distinct pattern of green fluorescence around the cells. At 24 hrs of treatment, the fluorescence intensity around cells increased and with fluorescence not seen anywhere else in the cells. LDHA shared a similar expression time of expression as PXDN. The green fluorescence is seen in untreated cells, however after 24-hr treatment the intensity increases dramatically (*Figure 3.3.).* LDHA expression is seen in the cytoplasm, and over time the FIT-C fluorescence intensity increases within the cells. Overall, these results (*Figure 3.1.-3.3.*) show that $CoCl_2$ treatment does alter the expression of HIF-1α, PXDN and LDHA. HIF-1α expression is increased after 3hrs of treatment and localises to the nuclei of HeLa cells, whereas PXDN and LDHA expression is greatly increased after 24 hrs of $CoCl_2$ treatment, with the proteins localising to the ECM and the cytoplasm, respectively.

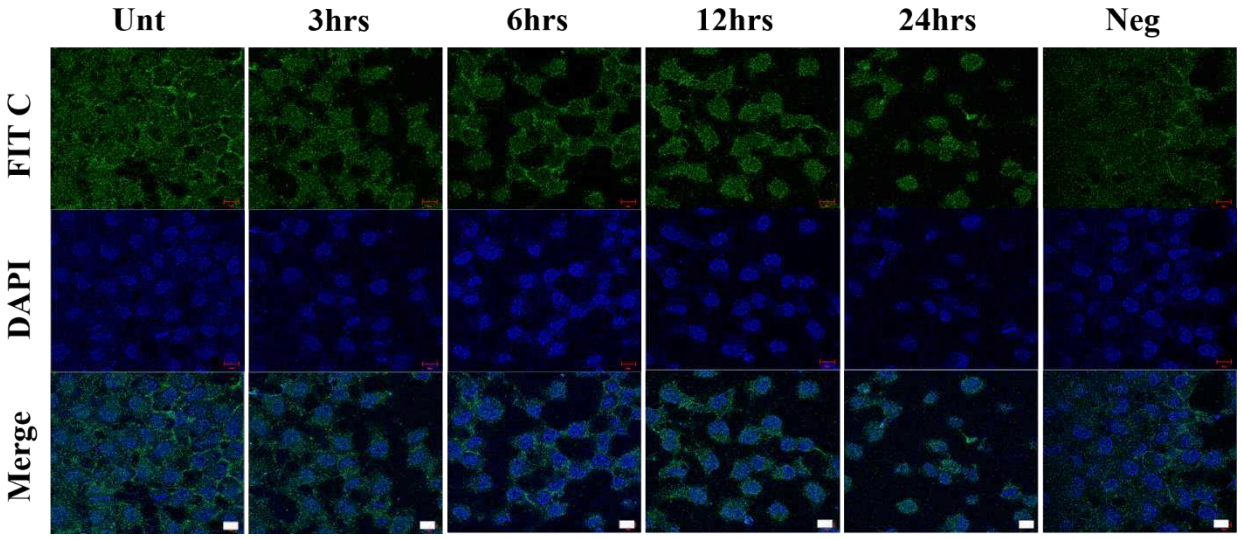

Figure 3.1. HIF-1a localises to the nucleus when the proteins expression is induced by treatment with $CoCl_2$. *HeLa cells were grown on coverslips and treated with $CoCl_2$ for 3hrs, 6hrs, 12hrs and 24hrs. The expression and localisation of HIF-1α was detected using a FIT C-conjugated secondary antibody and observed by confocal microscopy. HIF-1α accumulation in the cytoplasm is seen after 3hrs treatment, and the protein localises to the HeLa nuclei as $CoCl_2$ treatment is prolonged. (Magnification = 63x; Scale = 10µm).*

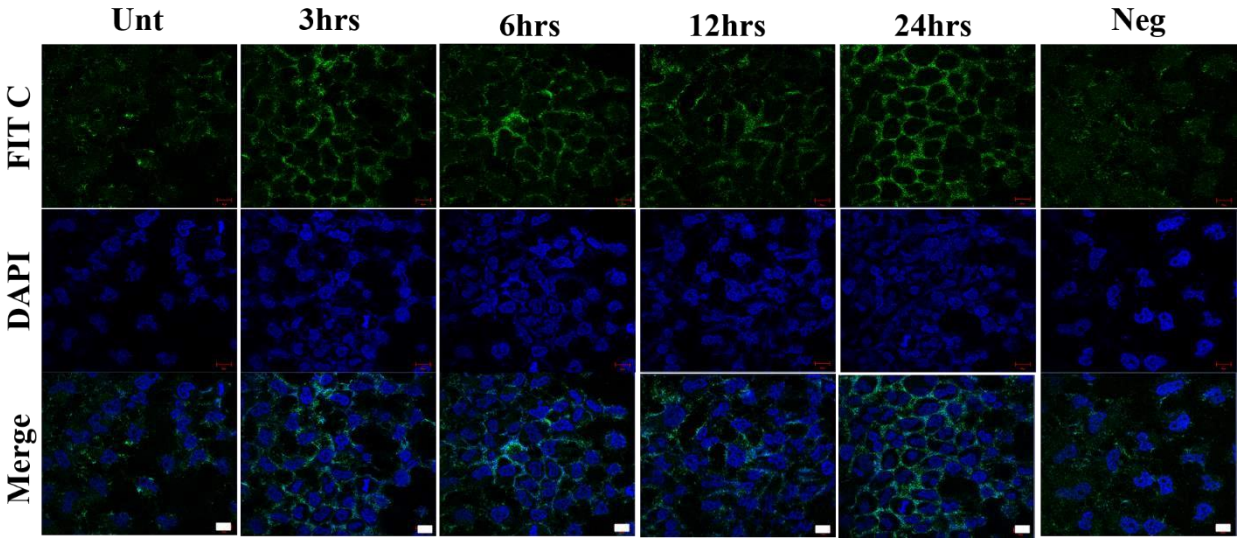

Figure 3.2. PXDN protein localises to the ECM of HeLa cells upon treatment with $CoCl_2$. *Cells were grown on glass coverslips and treated after 24hrs with $CoCl_2$ for 3hrs, 6hrs, 12hrs and 24hrs. The cells were then fixed and permeabilised before PXDN localisation and expression was determined with a FIT C-conjugated secondary antibody. PXDN localisation can be observed around the cells and its expression increases with longer treatments of $CoCl_2$; the highest intensity is seen at 24hrs. (Magnification = 63x; Scale = 10µm).*

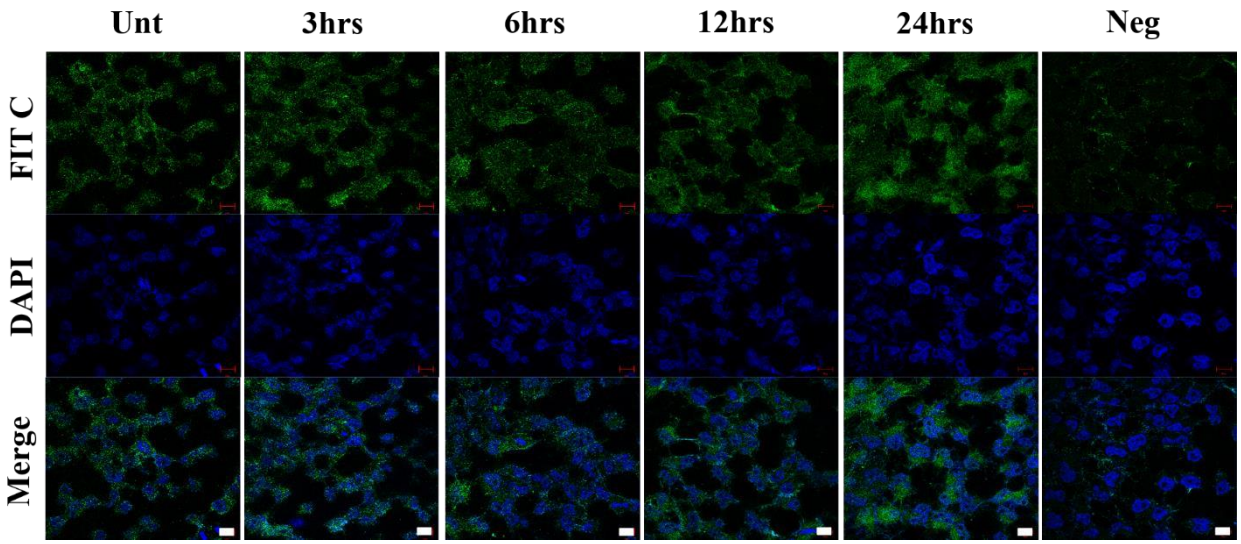

Figure 3.3. LDHA expression increases in HeLa cells after 24hr treatment with $CoCl_2$. *Cells were grown on glass coverslips and treated after 24hrs with $CoCl_2$ for 3hrs, 6hrs, 12hrs and 24hrs. The cells were then fixed and permeabilised before LDHA localisation and expression was determined with a FIT C-conjugated secondary antibody. LDHA protein is present in the cytoplasm and nuclei of HeLa cells prior to treatment and the fluorescence intensity observed remains similar up until the 12hrs treatment. After treatment for 24hrs, increased fluorescence is observed within cells. From this, LDHA is localised to the cytoplasm and nucleus (Magnification = 63x; Scale = 10µm).*

Next, we quantified the HIF-1α, PXDN and LDHA protein amounts found in HeLa whole cell lysates after $CoCl_2$ treatment. The Western blot technique was used after treating cells at the same time points as before. *Figure 3.4.* shows the protein bands and protein amounts quantified from HeLa cell lysates. At 0 hrs HIF-1α protein was undetectable, however from 3 hrs HIF-1α protein amounts increased and remained significantly elevated. As there was no band for the untreated sample, protein amounts for the treated time points were calculated relative to one another and presented in arbitrary densitometric units. PXDN protein produced bands for each time point; however, the protein amount quantified were only significant at the 24-hr treatment point. After 24 hrs, cell lysates had protein amount 3.4-fold higher as compared to the untreated samples. The changes in LDHA protein observed were not significant across all the time points. These results confirm the immunofluorescence microscopy as the changes in the graphs across the

different time points mimicked the expression patterns seen in the fluorescently labelled cells.

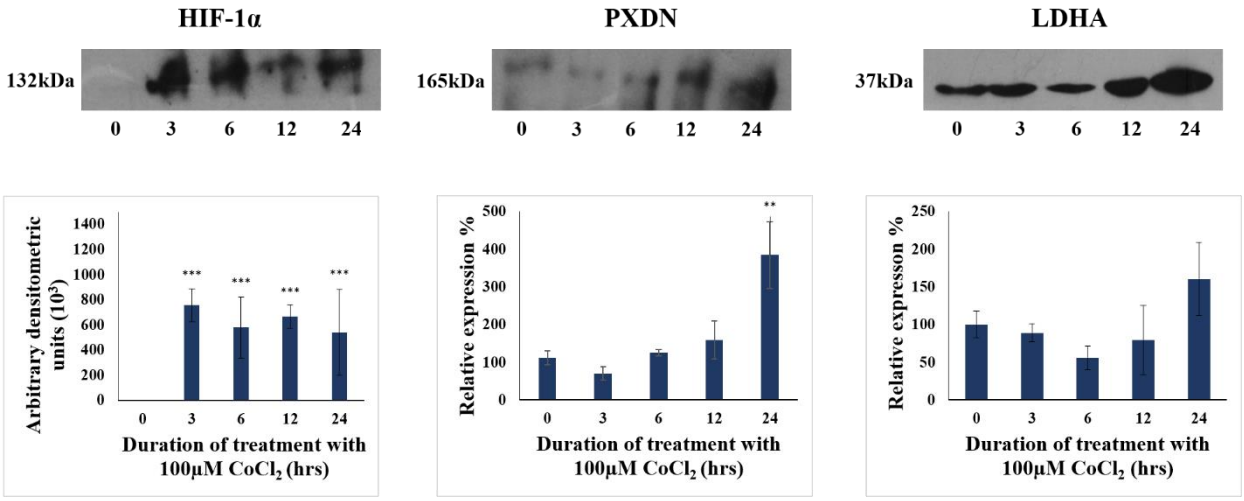

Figure 3.4. Western blot analysis shows that HIF-1α and PXDN expression is altered significantly after $CoCl_2$ treatment. *Cells were treated with 100µM $CoCl_2$ for 3hrs, 6hrs, 12hrs and 24hrs. HIF-1α, PXDN and LDHA protein was detected in whole-cell lysates, with elevated HIF-1α from 3 hours onwards, PXDN significantly higher at 24 hours, and LDHA higher at 24 hours but not significant. (n=3±SD) and significance determined using a Student's t-test, where p<0.05 was considered statistically significant. (**= P 0.01 and ***= P 0.001).*

Finally, we observed the interactions between HIF-1α and the *pxdn* promoter region using ChIP. First, we used the bioinformatic tool JASPAR, as well as a manual word search to identify putative HRE sites in the *pxdn* promoter region. (*Figure 3.5*.). Three putative binding sites ($PXDN^{HIF\text{-}1\alpha+}1$, $PXDN^{HIF\text{-}1\alpha+}2$ and $PXDN^{HIF\text{-}1\alpha+}3$) containing the consensus sequence 5′-ACGTG-3′ were found 1000bp upstream the *pxdn* promoter region (Wang *et al*, 1995). The third putative binding site contained two consensus sequences; however, they were not separable as they were closely situated therefore, we classified this as a single binding site. A region that lacked the consensus sequence was also chosen as a negative control for the experiments ($PXDN^{HIF\text{-}1\alpha-}$). LDHA remained our positive control for the ChIP experiments. The LDHA HRE binding site has previously been identified and was used as given by Luo *et al*, 2011 and Qui *et al*, 2014. A negative binding site was also included for the

control, together the LDHA positive and negative HRE sites identified were labelled LDHA$^{HIF\text{-}1\alpha+}$ and LDHA$^{HIF\text{-}1\alpha-}$, respectively.

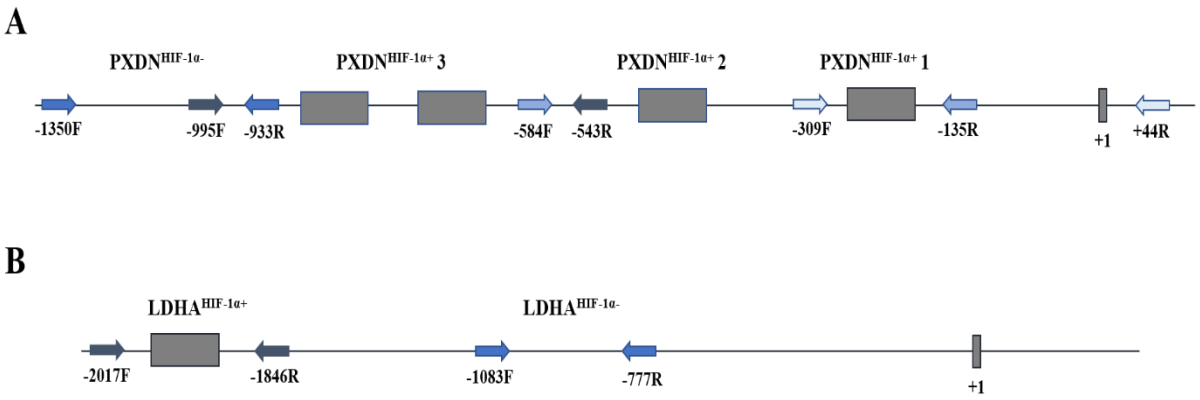

Figure 3.5. Bioinformatic analysis to determine putative HRE sites in the pxdn promoter region. A) *Three putative sites were identified in the pxdn promoter region (PXDN$^{HIF\text{-}1\alpha+}$1, PXDN$^{HIF\text{-}1\alpha+}$2 and PXDN$^{HIF\text{-}1\alpha+}$3). Primers were designed to cover each putative region (arrows)and a PXDNHIF-1 negative region.* ***B)*** *Ldha was used as a positive control (LDHA$^{HIF\text{-}1\alpha+}$) as the gene has a known HRE (Luo et al, 2011; Qui et al, 2014). A negative control region was also included for LDHA (LDHA$^{HIF\text{-}1\alpha-}$).*

After identifying these putative binding sites, we then tested the sonication protocol to ensure that the fragment sizes were correct and between 200 to 800 bp. The sonication gel is shown in *Figure 3.6.A.* Each primer was then first tested using gDNA (*Figure 3.6.B*). All the primers worked for the PCR reaction run on gDNA (*Figure 3.6. B*). The samples were then tested for ChIP by running PCR on fragmented DNA, of these samples only the PXDN$^{HIF\text{-}1\alpha+}$1 primer pair produced a faint band for both treated and untreated HeLa cells (*Figure 3.6.C*). The pair amplified across a region (-995 bp and -543 bp) that contained two putative binding sites for HIF-1. PCR products amplified from the ChIP assays show that in the putative *pxdn* region untreated cells (lane 1) show no amplification of the putative HRE region, however in the treated sample (lane 2) a faint band is seen showing that HIF-1 does bind the promoter region at this point. The negative control region for PXDN showed no amplification except for in the input control. For LDHA, the positive control

produced bands as expected; however, the negative control also produced faint bands for the treated and control regions and this was not expected. The remaining PXDN$^{HIF\text{-}1+}$ putative sites produced negative results. No bands were seen in the untreated or treated samples for these regions (*Figure 3.5.; Figure 3.6. D.*).

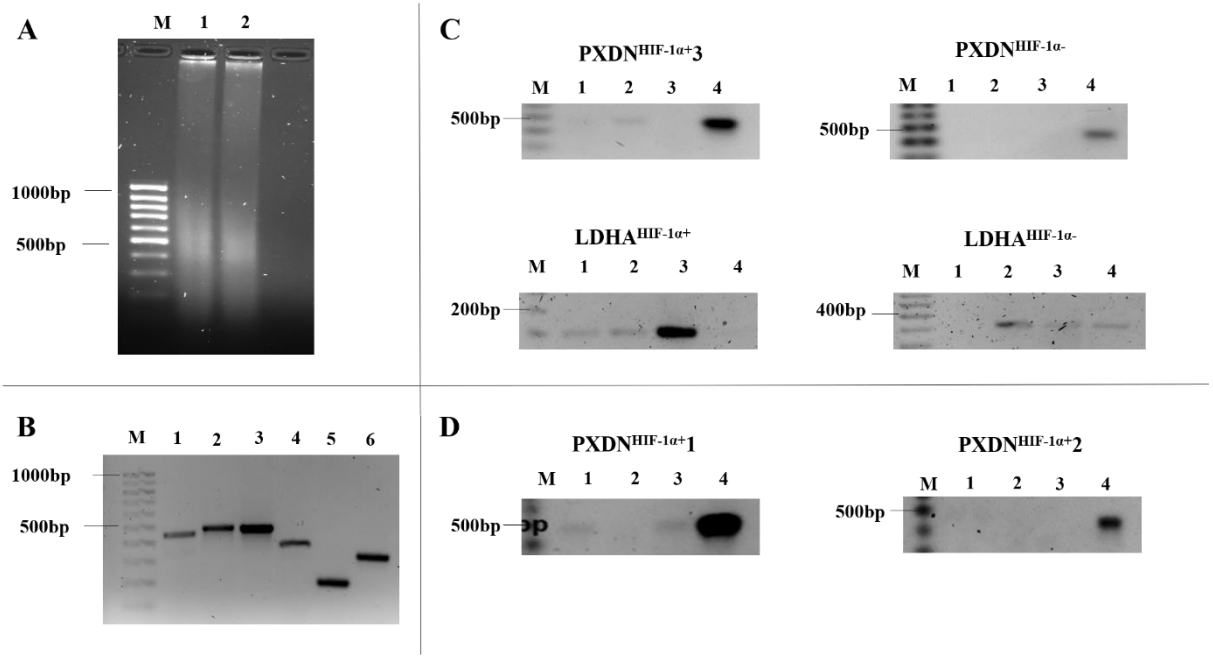

Figure 3.6. The pxdn promoter region contains an HRE that is bound by HIF-1. *ChIP was carried out to determine whether pxdn contains an HRE.* ***A).*** *Sonication gel: Untreated and treated HeLa cells we harvested and sonicated for 5 minutes at 40% amplitude and then electrophoresed on a 1.5% agarose gel. The majority of DNA fragment sizes ranged from 300bp-800bp. M- Molecular weight marker; 1- Untreated; 2-Treated.* ***B)****. Primer sets for each putative region were tested on gDNA. M - Molecular weight marker; 1 - PXDN^{HIF1-} (441bp); 2 - PXDN$^{HIF\text{-}1+}$1 (476bp); 3 - PXDN$^{HIF\text{-}1+}$2 (471bp); 4 - PXDN$^{HIF\text{-}1+}$3 (372bp); 5 - LDHA$^{HIF\text{-}1+}$(197bp); 6 - LDHA$^{HIF\text{-}1-}$ (326bp).* ***C and D)****. ChIP results for PXDN$^{HIF\text{-}1+}$, PXDN^{HIF-}, LDHA$^{HIF\text{-}1+}$ and LDHA$^{HIF\text{-}1-}$. For PXDN, M – Molecular weight marker, 1-Untreated, 2 - 100µM $CoCl_2$, 3 – No antibody control, 4 – Input control. For LDHA, M- Molecular weight marker, 1- Untreated, 2 -100µM $CoCl_2$, 3 – Input control, 4 – No antibody control.*

4. DISCUSSION

The maintenance of oxygen homeostasis is crucial for the survival of aerobic organisms (Semenza *et al*, 1996). Oxygen acts as the final electron acceptor in the electron transport chain during a process known as oxidative phosphorylation (Lopez-Barneo *et al*, 2001). The products of oxidative phosphorylation are chemical energy in the form of ATP and oxygen, reacts with H+ to form water (Lopez-Barneo *et al*, 2001). The oxygen produced is now available for the aerobic metabolism of various endogenous and exogenous substrates, including amino acids, lipids and catecholamines, amongst others (Vafhakha and Gilany, 2010). Prolonged disruptions in oxygen balance results in cellular changes that may lead to disease. These changes include the production of proteins responsible for the regulation of glucose metabolism and vascularisation, and may include response to damage to the basement membrane through the disruption of oxygen homeostasis (Semenza *et al*, 1996). Acute changes in oxygen homeostasis are rapidly detected, prompting the activation of HIF-1, the master regulator of cellular response to hypoxia. In this dissertation, we show that HIF-1 interacts with *pxdn*, a protein crucial for the maintenance of basement membrane integrity.

In endothelial cells, myofibroblasts and epithelial cells, PXDN is secreted into the ECM where it catalyses the crosslinking of collagen IV fibres – the major structural protein of the ECM (Nelson *et al*, 1994; Bhave *et al*, 2012; Pertefi and Geiszt, 2014). Therefore, the loss of membrane integrity and ECM structure caused by dysregulation of PXDN expression is a precursor for disease. The tissue damage seen in PXDN mediated kidney fibrosis, atherosclerosis, ASD, as well as the association between PXDN and cancer progression are continually being studied; however, the molecular mechanisms of PXDN expression and regulation remain elusive. Previously, Nrf2 the master regulator of cellular response to oxidative stress has been shown to regulate the transcription of *pxdn* in cervical cancer cell lines (Hanmer and Mavri-Damelin, 2018). Furthermore, PXDN plays a role in epithelial-mesenchymal transition in cervical cancer and embryonic kidney

cells through its regulation by Snai1 (Sitole and Mavri-Damelin, 2018). These two bodies of work link PXDN to redox-related changes in cellular function and differentiation that leads to the development of disease.

In our search to understand the role PXDN may play in cells affected by hypoxia and its possible regulation by HIF-1α, we identified putative HREs in the *pxdn* promoter. HREs are regions of 50 bp or less in the promoters or enhancers of HIF responsive genes and have a consensus sequence 5'-ACGTG-3' (Semenza *et al*, 1992). *Erythropoietin* and *VEGF* HREs were the first to be described, each containing HIF-1 binding sites of 33bp and 35bp, respectively (Semenza *et al*, 1991; Liu *et al*, 1995). Here we describe four putative HRE sites containing the above-mentioned sequence found 1000bp upstream the transcription start site (*Figure 3.5.*). HIF-1 binds HRE sequences, however the flanking sequences are essential for transcription of HIF responsive genes (Semenza *et al*, 1997). We chose LDHA as the positive control for HIF-1 regulation as *ldha* has been identified as a HIF responsive gene (Firth *et al*, 1994).

Once we had determined that *pxdn* contained putative HIF-1α binding sites, we observed the protein expression and localisation of PXDN in HeLa cells. In this case, our focus was on the HIF-1α subunit of HIF-1 as its expression is continually regulated by PHDs, whereas the HIF-1β subunit is constitutively expressed (Wang *et al*, 1995). HIF-1 expression in cells is usually driven by decreased oxygen availability; however, the protein may also be activated by non-hypoxic mechanism. In HeLa cells, an increased expression of HIF-1α was observed after treatment with $CoCl_2$. Although the cells were not maintained in hypoxic conditions, treatment of the cell culture media with $CoCl_2$ was used as a chemical hypoxia model. $CoCl_2$ stabilises HIF-1α in the cytoplasm by inhibiting the action of PHDs, this results in the translocation of the alpha subunit into the nucleus where it subsequently interacts with HIF-1β (Maxwell and Salnikow, 2003). In our experiments, HIF-1α nuclear localisation occurred between 3-6 hrs after treatment. The activation of HIF-1 in response to hypoxia varies depending on cell type and various other factors,

however multiple studies show that once degradation of the HIF-1α subunit is inhibited, the HIF-1 protein takes approximately 4 hrs to stabilise (Zhou *et al*, 2011). As such, our model correlates with what has been previously reported in literature. The expression and localisation of PXDN after treatment of HeLa cells with $CoCl_2$, showed that the PXDN protein localised to the ECM of the cells over a period of 24 hrs, although a distinct pattern of fluorescence in the ECM was identified from about 3 hrs of treatment. However, the changes in PXDN expression assessed by Western blot were only significant at the 24-hr time point. LDHA expression was increased in HeLa cells treated with $CoCl_2$. This was expected as *ldha* is a known target of HIF-1. HIF-1 activation leads to the expression of multiple glycolytic enzymes including GLUT1, aldolase A (ALDA), enolase 1 (ENO1), PGK1 and LDHA (Semenza *et al*, 1996). LDHA, in particular is a key enzyme in the glycolytic process responsible for the conversion of L-lactate to pyruvate (Cui *et al*, 2017). This interconversion is responsible for the anaerobic glycolysis characteristic of the hypoxic tumour environment known as the Warburg effect (Cui *et al*, 2017). The metabolic role of LDHA expression through the HIF-1 pathway has been observed in multiple cancers. In ovarian and pancreatic cancer cells LDHA was widely expressed in the cytoplasm, with increased activation of the *ldha* gene being associated with the progression and growth of tumours (Cui *et al*, 2017; Tang *et al*, 2016). Interestingly, we observed a rapid increase in LDHA expression in HeLa cells where significant changes were noted as early as three hours after treatment. This may be because LDHA protein expression is part of a central metabolic pathway and is constitutively expressed in multiple cells. Furthermore, LDHA is expressed in the cytoplasm with less cellular modification required. PXDN expression is widespread but PXDN protein expression is limited to endothelial cells, lens epithelium and myofibroblasts. In addition to this, PXDN is secreted into the ECM thus the molecular processing post-transcriptional modifications required for extra-cellular signalling may account for the increased time of localisation to the ECM.

Finally, we show that HIF-1 α binds the *pxdn* promoter region and may drive the transcription of the gene. Of the four putative binding sites, two sites could

not be differentiated by PCR as they were in close proximity. This region found between 741 bp and 801 bp upstream the transcription start site is where HIF-1α binds the *pxdn* promoter contains two HRE sites. Although the HRE is crucial for HIF-1 binding, sometimes a single HRE is insufficient for transcription activation of the target gene. *EPO* and *VEGF* contain a single HRE, however, *ENO1, Ldha* and *PGK1*promoter regions contain two HREs (Semenza *et al*, 1991; Liu *et al*, 1995; Semenza *et al*, 1996). As previously mentioned, the presence of an HRE site is necessary for HIF-1 binding yet this does not imply transcription of the bound gene. The additional flanking site may be necessary for the recruitment of transcription co factors. In this regard, the results presented are lacking as only the binding of HIF-1 to the *pxdn* promoter region has been shown. To determine the functionality of the *pxdn* HRE testing the transcriptional expression of PXDN by HIF-1α will be necessary, this may be achieved by using a luciferase assay.

To our knowledge, this is the first report of an HRE in the *pxdn* gene, as well as the first description of the relationship between HIF-1α and PXDN expression in HeLa cells through the non-hypoxic pathway. The transcriptional activation of genes by HIF-1 is an adaptive response to changing cellular microenvironment in the attempt to restore oxygen homeostasis, therefore this work provides a new framework for PXDN expression in physiological processes and in disease. HIF-1α is associated with the shift in expression of developmental genes during embryogenesis (Madan *et al*, 2002; Koblits *et al*, 2015). HIF-1α expression in the human brain, heart, kidney and liver is seen in early development of the human foetus (Madan et al, 2002). In the case of *EPO* gene expression during foetal development the protein is expressed in the liver, however this switch to expression in the kidney (Madan *et al*, 2002). Although Madan *et al* (2002) reported that HIF-1α itself was not responsible for the change in *EPO* tissue expression, HIF-1 itself coordinates the hypoxic environment responsible for the gene expression switching seen in developmental processes (Madan *et al*, 2002; Koblits *et al*, 2015). The interaction between HIF-1 and *pxdn* allows for the hypothesis that the coordination of the hypoxic environment in eye and cardiovascular

development. PXDN is expressed in developing murine and human lens epithelium playing a role in ROS homeostasis (Khan *et al*, 2011; Choi *et al*, 2015). HIF-1α transcriptional regulation of the PXDN gene may regulate the generation of ROS species in the developing eye. In disease, PXDN is associated with ischemia, atherosclerosis and the kidney fibrosis – process that require the activation of HIF responsive genes such as *VEGF* and *Snai1*.

The roles of HIF-1α and PXDN in cancer have both been previously described. Here we show a direct correlation between the expression of HIF-1α and PXDN in HeLa cervical cancer cells. PXDN is expressed in multiple cancers where it plays a role in ROS regulation as well as EMT. The progression and growth of tumours results in the need for increased metabolic needs and space. HIF-1 controls the glycolytic changes in cellular metabolism within the tumour cells as well as the increased blood vessel supply to the tumour microenvironment. We propose that the association between HIF-1 and *pxdn* suggest that the increased PXDN expression seen alongside increased HIF-1 expression may be responsible for the deposition of ECM in metastasizing cancer cells. Although decreased PXDN expression has been previously associated with the expression of the HIF responsive *Snai1*, it is possible that this may be a separate event present in the expression of PXDN in the early stages of the metastatic cascade (Sitole and Mavri-Damelin, 2018).

In conclusion, we present the first data showing that *pxdn* is a HIF-1 responsive gene, giving further insight into the regulation and function of PXDN. PXDN expression and regulation is essential in ECM structural integrity in multiple tissues. Furthermore, the role of both HIF-1α and PXDN in development, cardiovascular disease and cancer suggests that this interaction should be further explored for the development of novel therapeutics.

REFERENCES

Bai, Y.-P., Hu, C.-P., Yuan, Q., Peng, J., Shi, R.-Z., Yang, T.-L., Cao, Z.-H., Li, Y.-J., Cheng, G., Zhang, G.-G. (2011). Role of VPO1, a newly identified heme containing peroxidase, in ox-LDL induced endothelial cell apoptosis. *Free Radical Biology and Medicine.* **51**, 1492–1500.

Bathish, B., Kettle, A., Winterbourn, C. (2015). Inhibition of Peroxidasin-Mediated Collagen IV Crosslinking. *Free Radical Biology and Medicine.* **S1**, S109.

Bathish, B., Turner, R., Kettle, T., Winterbourn, C. (2016). Peroxidasin-Catalysed Oxidative Modifications of Proteins in the Extracellular Matrix. *Free Radical Biology and Medicine*. **100**, S19–S20.

Bathish, B., Turner, R., Paumann-Page, M., Kettle, A.J., Winterbourn, C.C. (2018). Characterisation of peroxidasin activity in isolated extracellular matrix and direct detection of hypobromous acid formation. *Archives of Biochemistry and Biophysics*. **646**, 120–127.

Battistuzzi, G., Bellei, M., Bortolotti, C.A. and Sola, M., 2010. Redox properties of heme peroxidases. *Archives of Biochemistry and Biophysics*, **500**(1), 21-36.

Bhave, G., Cummings, C.F., Vanacore, R.M., Kumagai-Cresse, C., Ero-Tolliver, I.A., Rafi, M., Kang, J.-S., Pedchenko, V., Fessler, L.I., Fessler, J.H., Hudson, B.G. (2012). Peroxidasin forms sulfilimine chemical bonds using hypohalous acids in tissue genesis. *Nature Chemical Biology*. **8**, 784–790.

Brandes, R.P. (2011). Vascular peroxidase 1/peroxidasin: a complex protein with a simple function? *Cardiovascular Research*. **91**, 1–2.

Bramhall, S., Noack, N., Wu, M. and Loewenberg, J.R. (1969). A simple colorimetric method for determination of protein. *Analytical biochemistry*. 31, 146-148.

Briem, E., Budkova, Z., Sigurdardottir, A.K., Hilmarsdottir, B., Kricker, J., Timp, W., Magnusson, M.K., Traustadottir, G.A., Gudjonsson, T. (2019). MiR-203a is differentially expressed during branching morphogenesis and EMT in breast progenitor cells and is a repressor of peroxidasin. *Mechanisms of Development*.
155, 34–47.

Campbell, S.E. and Katwa, L.C. (1997). Angiotensin II stimulated expression of transforming growth factor-β1in cardiac fibroblasts and myofibroblasts. *Journal of molecular and cellular cardiology*. **29** (7), 1947-1958.

Chapman-Smith, A., Lutwyche, J.K., Whitelaw, M.L. (2004). Contribution of the Per/Arnt/Sim (PAS) domains to DNA binding by the basic helix-loop-helix PAS transcriptional regulators. *The Journal of Biological Chemistry*. 279, 5353–5362.

Cheng, G., Li, H., Cao, Z., Qiu, X., McCormick, S., Thannickal, V.J., Nauseef, W.M., (2011). Vascular peroxidase-1 is rapidly secreted, circulates in plasma, and supports dityrosine cross-linking reactions. *Free Radical Biology and Medicine.* **51**, 1445–1453.

Cheng, G., Salerno, J.C., Cao, Z., Pagano, P.J., Lambeth, J.D. (2008a). Identification and characterization of VPO1, a new animal heme-containing peroxidase. *Free Radical Biology and Medicine.* **45**, 1682–1694.

Cheng, G., Salerno, J.C., Cao, Z., Pagano, P.J., Lambeth, J.D. (2008b). VPO1 and VPO2: identification and characterization of two new heme-containing peroxidases. *The FASEB Journal*. **22**, 611.26-611.26.

Choi, A., Lao, R., Tang, P.L.F., Wan, E., Mayer, W., Bardakjian, T., Shaw, G.M., Kwok, P.Y., Schneider, A. and Slavotinek, A. (2015). Novel mutations in PXDN cause microphthalmia and anterior segment dysgenesis. *European Journal of Human Genetics*, **23**(3), 337–341.

Choi, J.J., Ting, C.T., Trogrlic, L., Milevski, S.V., Familari, M., Martinez, G. and de Iongh, R.U. (2014). A role for smoothened during murine lens and cornea development. *PLoS One.* **9**(9), 108037.

Chistiakov, D.A., Melnichenko, A.A., Myasoedova, V.A., Grechko, A.V. and Orekhov, A.N. (2017). Mechanisms of foam cell formation in atherosclerosis. Journal of Molecular Medicine, **95**(11), 1153-1165.

Colon, S., and Bhave, G. (2016). Proprotein Convertase Processing Enhances Peroxidasin Activity to Reinforce Collagen IV. *The Journal of Biological Chemistry*. **291**, 24009–24016.

Colon, S., Luan, H., Liu, Y., Meyer, C., Gewin, L., Bhave, G. (2018). Peroxidasin and eosinophil peroxidase, but not myeloperoxidase, contribute to renal

fibrosis in the murine unilateral ureteral obstruction model. *American Journal of Physiology Renal Physiology* **316**, F360–F371.

Conway, E.M., Collen, D. and Carmeliet, P. (2001). Molecular mechanisms of blood vessel growth. *Cardiovascular research.* **49**(3), 507-521.

Cui, S., Lv, X., Li, W., Li, Z., Liu, H., Gao, Y., Huang, G. (2018). Folic acid modulates VPO1 DNA methylation levels and alleviates oxidative stress-induced apoptosis in vivo and in vitro. *Redox Biology* **19**, 81–91.

Denco, N.C. (2008). Hypoxia, HIF1 and glucose metabolism in the solid tumor. *Nature Rev Cancer*. **8**, 705-707.

Dengler, V.L., Galbraith, M.D., Espinosa, J.M. (2014). Transcriptional regulation by hypoxia inducible factors, Critical Reviews in Biochemistry and Molecular Biology, (49)1, 1-15.Dougan, J., Hawsawi, O., Burton, L.J., Edwards, G., Jones, K., Zou, J., Nagappan, P., Wang, G., Zhang, Q., Danaher, A., Bowen, N., Hinton, C., Odero-Marah, V.A., (2019). Proteomics-Metabolomics Combined Approach Identifies Peroxidasin as a Protector against Metabolic and Oxidative Stress in Prostate Cancer.*International Journal of Molecular Sciences*. **20**, 3046.

Ero-Tolliver, I.A., Hudson, B.G., Bhave, G. (2015). The Ancient Immunoglobulin Domains of Peroxidasin Are Required to Form Sulfilimine Cross-links in Collagen IV. *The Journal of Biological Chemistry*. **290**, 21741–21748.

Fidler, A.L., Vanacore, R.M., Chetyrkin, S.V., Pedchenko, V.K., Bhave, G., Yin, V.P., Stothers, C.L., Rose, K.L., McDonald, W.H., Clark, T.A. and Borza, D.B. (2014). A unique covalent bond in basement membrane is a primordial innovation for tissue evolution. *Proceedings of the National Academy of Sciences.* **111**(1), 331-336.

Gábor, S., Hajnal, K.A., Enikő, L., Krisztina, K., Ágnes, D., Balázs, E., Grasberger, H., Miklós, G. (2018). Peroxidasin-mediated crosslinking of collagen IV is independent of NADPH oxidases. *Redox Biology*. **16**, 314–321.

Ge, L., Zhang, G., You, B., Cheng, G., Chen, L., Shi, R. (2017). The role of losartan in preventing vascular remodeling in spontaneously hypertensive rats by inhibition of the H2O2/VPO1/HOCl/MMPs pathway. *Biochemical and Biophysical Research Communications*. **493**, 855–861.

Geer, L.Y., Marchler-Bauer, A., Geer, R.C., Han, L., He, J., He, S., Liu, C., Shi, W. and Bryant, S.H., (2010). The NCBI biosystems database. *Nucleic acids research*. **38** (S1), D492–D496.

Gotenstein, J.R., Swale, R.E., Fukuda, T., Wu, Z., Giurumescu, C.A., Goncharov, A., Jin, Y., Chisholm, A.D. (2010). The C. elegans peroxidasin PXN-2 is essential for embryonic morphogenesis and inhibits adult axon regeneration. *Development*. **137**, 3603–3613.

Graw, J., Wagner, S., Fuchs, H., Angelis, M.H.D. (2011). Mutation in *Pxdn* encoding peroxidasin causes small lenses and kinky tails in the mouse. *Acta Ophthalmologica*. **89**.

Hanmer, K.L., Mavri-Damelin, D. (2018). Peroxidasin is a novel target of the redox sensitive transcription factor Nrf2. *Gene.* **674**, 104–114.

Horikoshi, N., Cong, J., Kley, N., Shenk, T. (1999). Isolation of Differentially Expressed cDNAs from p53-Dependent Apoptotic Cells: Activation of the Human Homologue of the Drosophila Peroxidasin Gene. *Biochemical and Biophysical Research Communications.* **261**, 864–869.

Janssen-Heininger, Y.M., Mossman, B.T., Heintz, N.H., Forman, H.J., Kalyanaraman, B., Finkel, T., Stamler, J.S., Rhee, S.G. and van der Vliet, A., 2008. Redox-based regulation of signal transduction: principles, pitfalls, and promises. *Free Radical Biology and Medicine*, **45**(1), 1 –17.

Jayachandran, A., Prithviraj, P., Lo, P.H., Walkiewicz, M., Anaka, M., Woods, B.L., Tan, B., Behren, A., Cebon, J. and McKeown, S.J., 2016. Identifying and targeting determinants of melanoma cellular invasion. *Oncotarget*, **7**(27), 41186.

Jiang, J., Wang, K., Chen, Y., Chen, H., Nice, E.C., Huang, C. (2017). Redox regulation in tumor cell epithelial–mesenchymal transition: molecular basis and therapeutic strategy. *Signal Transduction and Targeted Therapy.* **2**, 1–12.

Kallio, P.J., Okamoto, K., O'Brien, S., Carrero, P., Makino, Y., Tanaka, H. and Poellinger, L. (1998). Signal transduction in hypoxic cells: inducible nuclear translocation and recruitment of theCBP/p300 coactivator by the hypoxia-induciblefactor-1α. *The EMBO journal*, **17**(22), 6573-6586.

Kallio, P.J., Wilson, W.J., O'Brien, S., Makino, Y. and Poellinger, L. (1999). Regulation of the hypoxia-inducible transcription factor 1α by the ubiquitin-proteasome pathway. *Journal of Biological Chemistry*. **274**(10), 6519-6525.

Katsuno, Y., Lamouille, S. and Derynck, R. (2013). TGF-β signaling and epithelial–mesenchymal transition in cancer progression. *Current opinion in oncology*. **25**(1), 76-84.

Ke, Q., Costa, M. (2006). Hypoxia-inducible factor-1 (HIF-1). *Molecular Pharmacology*. **70**, 1469–1480.

Khan, A., Fornes, O., Stigliani, A., Gheorghe, M., Castro-Mondragon, J.A., van der Lee, R., Bessy, A., Chèneby, J., Kulkarni, S.R., Tan, G., Baranasic, D., Arenillas, D.J., Sandelin, A., Vandepoele, K., Lenhard, B., Ballester, B., Wasserman, W.W., Parcy, F., Mathelier, A. (2018). JASPAR 2018: update of the open-access database of transcription factor binding profiles and its web framework. *Nucleic Acids Research*. **46**, D260–D266.

Kher, N. and Marsh, J.D. (2004). Pathobiology of atherosclerosis. *Seminars in Thrombosis and Hemostasis.* **30,** 665-672.

Köblitz, L., Fiechtner, B., Baus, K., Lussnig, R. and Pelster, B. (2015). Developmental expression and hypoxic induction of hypoxia inducible transcription factors in the zebrafish. *PloS one*. **10**(6), 0128938.

Koh, M.Y., Lemos, R., Liu, X., Powis, G. (2011). The hypoxia-associated factor switches cells from HIF-1α- to HIF-2α-dependent signaling promoting stem cell characteristics, aggressive tumor growth and invasion. *Cancer Research*. **71**, 4015–4027.

Koh, M.Y., Powis, G. (2012). Passing the baton: the HIF switch. *Trends Biochemical Sciences*. **37**, 364–372.

Lázár, E., Péterfi, Z., Sirokmány, G., Kovács, H.A., Klement, E., Medzihradszky, K.F. and Geiszt, M. (2015). Structure–function analysis of peroxidasin provides insight into the mechanism of collagen IV crosslinking. *Free Radical Biology and Medicine*. **83**, 273-282.

Li, H., Cao, Z., Moore, D.R., Jackson, P.L., Barnes, S., Lambeth, J.D., Thannickal, V.J., Cheng, G. (2012a). Microbicidal Activity of Vascular Peroxidase 1 in

Human Plasma via Generation of Hypochlorous Acid. *Infection and Immunity*. **80**,2528–2537.

Li, H., Cao, Z., Zhang, G., Thannickal, V.J., Cheng, G. (2012b). Vascular peroxidase 1 catalyzes the formation of hypohalous acids: Characterization of its substrate specificityand enzymatic properties. *Free Radical Biology and Medicine.* **53**, 1954–1959.

Li, T., Peng, J.J., Wang, E.L., Li, N.S., Song, F.L., Yang, J.-F., Luo, X.-J., Liu, B., Peng, J. (2019). Magnesium Lithospermate B Derived from Salvia miltiorrhiza Ameliorates Right Ventricle Remodeling in Pulmonary Hypertensive Rats via Inhibition of NOX/VPO1 Pathway. *Planta Med.* **85**, 708–718.

Li, T.-T., Zhang, Y.-S., He, L., Liu, B., Shi, R.-Z., Zhang, G.-G., Peng, J. (2012). Inhibition of vascular peroxidase alleviates cardiac dysfunction and apoptosis induced by ischemia–reperfusion. *Canadian Journal of Physiology and Pharmacology.* **90**, 851–862.

Liu, B., Luo, X.-J., Yang, Z.-B., Zhang, J.-J., Li, T.-B., Zhang, X.-J., Ma, Q.-L., Zhang, G.-G., Hu, C.-P., Peng, J. (2014). Inhibition of NOX/VPO1 Pathway and Inflammatory Reaction by Trimethoxystilbene in Prevention of Cardiovascular Remodeling in Hypoxia-induced Pulmonary Hypertensive Rats. *Journal of Cardiovascular Pharmacology.* **63**, 567.

Liu, S.-Y., Yuan, Q., Li, X.-H., Hu, C.-P., Hu, R., Zhang, G.-G., Li, D., Li, Y.-J. (2015). Role of vascular peroxidase 1 in senescence of endothelial cells in diabetes rats. *International Journal of Cardiology*. **197**, 182–191.

Liu, Y., Li, Q., Zhou, L., Xie, N., Nice, E.C., Zhang, H., Huang, C., Lei, Y. (2016). Cancer drug resistance: redox resetting renders a way. *Oncotarget.* **7**, 42740–42761.

Liu, Z., Liu, Y., Xu, Q., Peng, H., Tang, Y., Yang, T., Yu, Z., Cheng, G., Zhang, G., Shi, R. (2017). Critical role of vascular peroxidase 1 in regulating endothelial nitric oxide synthase. *Redox Biology.* **12**, 226–232.

López-Barneo, J., Pardal, R. and Ortega-Sáenz, P. (2001). Cellular mechanism of oxygen sensing. *Annual review of physiology*. **63**(1), 259-287.

Luo, W., Hu, H., Chang, R., Zhong, J., Knabel, M., O'Meally, R., Cole, R.N., Pandey, A. and Semenza, G.L. (2011). Pyruvate kinase M2 is a PHD3-stimulated coactivator for hypoxia-inducible factor 1. *Cell*. **145**(5), 732-744.

Ma, Q.-L., Zhang, G.-G., Peng, J. (2013). Vascular peroxidase 1: A novel enzyme in promoting oxidative stress in cardiovascular system. *Trends in Cardiovascular Medicine.* **23**, 179–183.

Madan, A., Varma, S. and Cohen, H.J. (2002). Developmental stage-specific expression of the α and β subunits of the HIF-1 protein in the mouse and human fetus. *Molecular genetics and metabolism*. **75**(3), 244-249.

Mahon, P.C., Hirota, K. and Semenza, G.L. (2001). FIH-1: a novel protein that interacts with HIF-1α and VHL to mediate repression of HIF-1 transcriptional activity. *Genes & development.* **15** (20), 2675-2686.

Manral, P., Colon, S., Bhave, G., Zhao, M.-H., Jain, S., Borza, D.-B. (2019). Peroxidasin Is a Novel Target of Autoantibodies in Lupus Nephritis. *Kidney International Reports*. **4,** 1004–1006.

Maxwell, P. and Salnikow, K. (2004). HIF-1, an oxygen and metal responsive transcription factor. *Cancer biology & therapy*. **3**(1), 29-35.

McAdoo, S.P., Pusey, C.D. (2018). Peroxidasin—a Novel Autoantigen in Anti-GBM Disease? *Journal of the American Society of Nephrology.* **29,** 2605–2607.

McCall, A.S., Bhave, G., Pedchenko, V., Hess, J., Free, M., Little, D.J., Baker, T.P., Pendergraft, W.F., Falk, R.J., Olson, S.W., Hudson, B.G. (2018a). Inhibitory Anti-Peroxidasin Antibodies in Pulmonary-Renal Syndromes. *Journal of the American Society of Nephrology.* **29**, 2619–2625.

McCall, A.S., Bhave, G., Pedchenko, V., Hess, J., Free, M., Little, D.J., Baker, T.P., Pendergraft, W.F., Falk, R.J., Olson, S.W., Hudson, B.G. (2018b). Inhibitory Anti-Peroxidasin Antibodies in Pulmonary-Renal Syndromes. *Journal of the American Society of Nephrology.* **29**, 2619–2625.

Medfai, H., Khalil, A., Rousseau, A., Nuyens, V., Paumann-Page, M., Sevcnikar, B., Furtmüller, P.G., Obinger, C., Moguilevsky, N., Peulen, O., Herfs, M.,

Castronovo, V., Amri, M., Van Antwerpen, P., Vanhamme, L., Zouaoui and Boudjeltia, K. (2019). Human peroxidasin 1 promotes angiogenesis through ERK1/2, Akt, and FAK pathways. *Cardiovascular Research*. **115**, 463–475.

Mitchell, M.S., Kan-Mitchell, J., Minev, B., Edman, C., and Deans, R.J. (2000). A novel melanoma gene (MG50) encoding the interleukin 1 receptor antagonist and six epitopes recognized by human cytolytic T lymphocytes. *Cancer research*. **60**(22), 6448-6456.

Nelson, R.E., Fessler, L.I., Takagi, Y., Blumberg, B., Keene, D.R., Olson, P.F., Parker, C.G., and Fessler, J.H. (1994). Peroxidasin: a novel enzyme-matrix protein of Drosophila development. *The EMBO Journal*. **13**, 3438–3447.

Nihei, S., Yamashita, K., Tasaki, H., Ozumi, K., Nakashima, Y. (2005). Oxidized lowdensity lipoprotein-induced apoptosis is attenuated by insulin-activated phosphatidylinositol 3-kinase/Akt through p38 mitogen-activated protein kinase. *Clinical Experimental Pharmacological Physiology*. **32**:224–229.

O'Leary', N.A., Wright, M.W., Brister, J.R., Ciufo, S., Haddad, D., McVeigh, R., Rajput, B., Robbertse, B., Smith-White, B., Ako-Adjei, D. and Astashyn, A. (2016). Reference sequence (RefSeq) database at NCBI: current status, taxonomic expansion, and functional annotation. *Nucleic acids research*. **44** (D1), D733-D745.

Paumann-Page, M., Katz, R.-S., Bellei, M., Schwartz, I., Edenhofer, E., Sevcnikar, B., Soudi, M., Hofbauer, S., Battistuzzi, G., Furtmüller, P.G., Obinger, C. (2017). Pre-steady-state Kinetics Reveal the Substrate Specificity and Mechanism of Halide Oxidation of Truncated Human Peroxidasin 1. *The Journal of Biological Chemistry*. **292**, 4583–4592.

Paumann-Page, M., Tscheliessnig, R., Sevcnikar, B., Katz, R.-S., Schwartz, I., Hofbauer, S., Pfanzagl, V., Furtmüller, P.G., Obinger, C. (2020). Monomeric and homotrimeric solution structures of truncated human peroxidasin 1 variants. *Biochimica et Biophysica Acta (B Proteins and Proteomics*. **1868**, 140249.

Pchelintsev, N.A., Adams, P.D., Nelson, D.M. (2016). Critical Parameters for Efficient Sonication and Improved Chromatin Immunoprecipitation of High Molecular Weight Proteins. *PloS One.* **11**.

Peng, H., Chen, L., Huang, X., Yang, T., Yu, Z., Cheng, G., Zhang, G., Shi, R. (2016). Vascular peroxidase 1 up regulation by angiotensin II attenuates nitric oxide production through increasing asymmetrical dimethylarginine in HUVECs. *Journal of the American Society of Hypertension*. **10**, 741-751.e3.

Peng, H., Zhang, K., Liu, Z., Xu, Q., You, B., Li, C., Cao, J., Zhou, H., Li, X., Chen, J., Cheng, G., Shi, R., Zhang, G. (2018). VPO1 Modulates Vascular Smooth Muscle Cell Phenotypic Switch by Activating Extracellular Signal-regulated Kinase 1/2 (ERK 1/2) in Abdominal Aortic Aneurysms. *Journal of the American Heart Association*. **7**, e010069.

Péterfi, Z., Donkó, Á., Orient, A., Sum, A., Prókai, Á., Molnár, B., Veréb, Z., Rajnavölgyi, É., Kovács, K.J., Müller, V., Szabó, A.J., Geiszt, M. (2009). Peroxidasin Is Secreted and Incorporated into the Extracellular Matrix of Myofibroblasts and Fibrotic Kidney. *The American Journal of Pathology*. **175**, 725–735.

Péterfi, Z., Geiszt, M. (2014). Peroxidasins: novel players in tissue genesis. *Trends in Biochemical Sciences.* **39**, 305–307.

Salceda, S. and Caro, J. (1997). Hypoxia-inducible factor 1α (HIF-1α) protein is rapidly degraded by the ubiquitin-proteasome system under normoxic conditions Its stabilization by hypoxia depends on redox-induced changes. *Journal of Biological Chemistry*. **272**(36), 22642-22647.

Semenza, G.L. (2002). HIF-1 and tumor progression: pathophysiology and therapeutics. *Trends in Molecular Medicine*. **8**, S62–S67.

Semenza, G.L. (2002). Signal transduction to hypoxia-inducible factor 1. *Biochemical Pharmacology, Cell Signaling, Transcription and Translation as Therapeutic Targets*. **64**, 993–998.

Semenza, G.L. (2001). HIF-1 and mechanisms of hypoxia sensing. *Current Opinion in Cell Biology*. **13**, 167–171.

Semenza, G.L. (2000). Expression of hypoxia-inducible factor 1: mechanisms and consequences. *Biochemical Pharmacology*. **59**, 47–53.

Semenza, G.L. (1998). Hypoxia-inducible factor 1: master regulator of O2 homeostasis. *Current Opinion in Genetics & Development*. **8**, 588–594.

Semenza, G.L., Jiang, B.-H., Leung, S.W., Passantino, R., Concordet, J.-P., Maire, P., Giallongo, A. (1996). Hypoxia Response Elements in the Aldolase A, Enolase 1, and Lactate Dehydrogenase A Gene Promoters Contain Essential Binding Sites for Hypoxia-inducible Factor 1. *The Journal of Biological Chemistry*. **271**, 32529–32537.

Shi, R., Cao, Z., Li, H., Graw, J., Zhang, G., Thannickal, V.J., Cheng, G. (2018). Peroxidasin contributes to lung host defense by direct binding and killing of gramnegative bacteria. *PLOS Pathogens*. **14**, e1007026.

Shi, R., Hu, C., Yuan, Q., Yang, T., Peng, J., Li, Y., Bai, Y., Cao, Z., Cheng, G., Zhang, G. (2011). Involvement of vascular peroxidase 1 in angiotensin II-induced vascular smooth muscle cell proliferation. Cardiovascular Research. **91**, 27–36.

Sirokmány, G., Kovács, H.A., Lázár, E., Kónya, K., Donkó, Á., Enyedi, B., Grasberger, H. and Geiszt, M., (2018). Peroxidasin-mediated crosslinking of collagen IV is independent of NADPH oxidases. *Redox biology.* **16**, 314–321.

Sitole, B.N., Mavri-Damelin, D. (2018). Peroxidasin is regulated by the epithelialmesenchymal transition master transcription factor Snai1. *Gene*. **646**, 195–202.

Soni, S., Padwad, Y.S. (2017). HIF-1 in cancer therapy: two-decade long story of a transcription factor. *Acta Oncologica*. **56**, 503–515.

Soudi, M., Paumann-Page, M., Delporte, C., Pirker, K.F., Bellei, M., Edenhofer, E., Stadlmayr, G., Battistuzzi, G., Boudjeltia, K.Z., Furtmüller, P.G., Antwerpen, P.V., Obinger, C. (2015). Multidomain Human Peroxidasin 1 Is a Highly Glycosylated and Stable Homotrimeric High Spin Ferric Peroxidase. *The Journal of Biological Chemistry*. **290**, 10876–10890.

Takahashi, M., Okazaki, H., Ogata, Y., Takeuchi, K.; Ikeda, U.; Shimada, K. (2002). Lysophosphatidylcholine induces apoptosis in human endothelial cells through a p38-mitogen-activated protein kinase-dependent mechanism. *Atherosclerosis*. **161**:387–394.

Tang, Y., Xu, Q., Peng, H., Liu, Z., Yang, T., Yu, Z., Cheng, G., Li, X., Zhang, G., Shi, R. (2015). The role of vascular peroxidase 1 in ox-LDL-induced vascular smooth muscle cell calcification. *Atherosclerosis.* **243**, 357–363.

Tauber, S., Jais, A., Jeitler, M., Haider, S., Husa, J., Lindroos, J., Knöfler, M., Mayerhofer, M., Pehamberger, H., Wagner, O. and Bilban, M., 2010. Transcriptome analysis of human cancer reveals a functional role of heme oxygenase-1 in tumor cell adhesion. *Molecular cancer*. **9**(1), 200.

Tindall, A.J., Pownall, M.E., Morris, I.D., Isaacs, H.V. (2005). *Xenopus tropicalis* peroxidasin gene is expressed within the developing neural tube and pronephric kidney. *Developmental Dynamics*. **232**, 377–384.

Weinhouse, S. (1955). Oxidative metabolism of neoplastic tissues. In *advances in cancer research*. **3**, 269-325.

Woods, K. (2013). Abstract 3011: The role of peroxidasin in human prostate cancer. *Cancer Research*. **73**, 3011–3011.

Wykoff, C.C., Pugh, C.W., Maxwell, P.H., Harris, A.L. and Ratcliffe, P.J. (2000). Identification of novel hypoxia dependent and independent target genes of the von Hippel-Lindau (VHL) tumour suppressor by mRNA differential expression profiling. *Oncogene.* **19**(54), 6297-6305.

Yan, X., Sabrautzki, S., Horsch, M., Fuchs, H., Gailus-Durner, V., Beckers, J., Hrabě de Angelis, M., Graw, J. (2014). Peroxidasin is essential for eye development in the mouse. *Human Molecular Genetics*. **23**, 5597–5614.

Yang, L., Bai, Y., Li, N., Hu, C., Peng, J., Cheng, G., Zhang, G., Shi, R. (2013). Vascular VPO1 expression is related to the endothelial dysfunction in spontaneously hypertensive rats. *Biochemical and Biophysical Research Communications*. **439**, 511–516.

Yang, W., Liu, Z., Xu, Q., Peng, H., Chen, L., Huang, X., Yang, T., Yu, Z., Cheng, G., Zhang, G., Shi, R. (2017). Involvement of vascular peroxidase 1 in angiotensin II– induced hypertrophy of H9c2 cells. *Journal of the American Society of Hypertension*. **11**, 519-529.e1.

Yang, Y., Cao, Z., Tian, L., Garvey, W.T., Cheng, G. (2013). VPO1 Mediates ApoE Oxidation and Impairs the Clearance of Plasma Lipids. *PLOS ONE*. **8**, e57571.

Yang, Y., Shi, R., Cao, Z., Zhang, G., Cheng, G., 2016. VPO1 mediates oxidation of LDL and formation of foam cells. *Oncotarget* **7**, 35500–35511.

You, B., Liu, Y., Chen, J., Huang, X., Peng, H., Liu, Z., Tang, Y., Zhang, K., Xu, Q., Li, X., Cheng, G., Shi, R., Zhang, G. (2018). Vascular peroxidase 1

mediates hypoxia-induced pulmonary artery smooth muscle cell proliferation, apoptosis resistance and migration. *Cardiovascular Research*. **114**, 188–199.

Zamocky, M., Jakopitsch, C., Furtmüller, P.G., Dunand, C. and Obinger, C. (2008). The peroxidase–cyclooxygenase superfamily: reconstructed evolution of critical enzymes of the innate immune system. *Proteins: Structure, Function, and Bioinformatics*, **72**(2), 589–605.

Zhang, Y.-S., He, L., Liu, B., Li, N.-S., Luo, X.-J., Hu, C.-P., Ma, Q.-L., Zhang, G.-G., Li, Y.-J., Peng, J. (2012). A novel pathway of NADPH oxidase/vascular peroxidase 1 in mediating oxidative injury following ischemia–reperfusion. *Basic Research in Cardiology*. **107**, 266.

Zhou, W., Dosey, T.L., Biechele, T., Moon, R.T., Horwitz, M.S. and Ruohola Baker, H., (2011). Assessment of hypoxia inducible factor levels in cancer cell lines upon hypoxic induction using a novel reporter construct. *PloS one*. **6**(11), 27460.

Ziello, J.E., Jovin, I.S., Huang, Y. (2007). Hypoxia-Inducible Factor (HIF)-1 Regulatory Pathway and its Potential for Therapeutic Intervention in Malignancy and Ischemia. *Yale Journal Biological Medicine*. **80**, 51–60.